# A new terrestrial biosphere model with coupled carbon, nitrogen, and phosphorus cycles (QUINCY v1.0; revision 1772)

Tea Thum[1], Silvia Caldararu[1], Jan Engel[1], Melanie Kern[1,2,3], Marleen Pallandt[1,2], Reiner Schnur[4], Lin Yu[1], and Sönke Zaehle[1,5]

[1]Max Planck Institute for Biogeochemistry, Hans-Knöll Str. 10, 07745 Jena, Germany
[2]International Max Planck Research School (IMPRS) for Global Biogeochemical Cycles, Jena, Germany
[3]Technical University Munich - School of Life Sciences, Weihenstephan, Germany
[4]Max Planck Institute for Meteorology, Hamburg, Germany
[5]Michael Stifel Center Jena for Data-driven and Simulation Science, Jena, Germany

**Correspondence:** Tea Thum (tthum@bgc-jena.mpg.de), Sönke Zaehle (szaehle@bgc-jena.mpg.de)

**Abstract.** The dynamics of terrestrial ecosystems are shaped by the coupled cycles of carbon, nitrogen and phosphorus, and strongly depend on the availability of water and energy. These interactions shape future terrestrial biosphere responses to global change. Many process-based models of the terrestrial biosphere have been gradually extended from considering carbon-water interactions to also including nitrogen, and later, phosphorus dynamics. This evolutionary model development has hindered full integration of these biogeochemical cycles and the feedbacks amongst them. Here we present a new terrestrial ecosystem model QUINCY (QUantifying Interactions between terrestrial Nutrient CYcles and the climate system), which is formulated around a consistent representation of element cycling in terrestrial ecosystems. This new model includes i) a representation of plant growth which separates source (e.g. photosynthesis) and sink (growth rate of individual tissues, constrained by nutrients, temperature, and water availability) processes; ii) the acclimation of many ecophysiological processes to meteorological conditions and/or nutrient availabilities; iii) an explicit representation of vertical soil processes to separate litter and soil organic matter dynamics; iv) a range of new diagnostics (leaf chlorophyll content; $^{13}$C, $^{14}$C, and $^{15}$N isotope tracers) to allow for a more in-depth model evaluation. We present the model structure and provide an assessment of its performance against a range of observations from global-scale ecosystem monitoring networks. We demonstrate that the framework is capable of consistently simulating ecosystem dynamics across a large gradient in climate and soil conditions, as well as across different plant functional types. To aid this understanding we provide an assessment of the model's sensitivity to its parameterisation and the associated uncertainty.

## 1 Introduction

Past, present, and future changes in climatic conditions and atmospheric $CO_2$ concentrations affect terrestrial vegetation and soils (Hou et al., 2018; De Kauwe et al., 2013; Swann et al., 2016), which in turn provide biogeophysical and biogeochemical feedbacks to the atmosphere (Bonan, 2008; Friedlingstein et al., 2014; Zaehle et al., 2010). To predict the likely trajectories of terrestrial ecosystems under climate change and their climate feedbacks, it is important to develop and test advanced modelling tools for the terrestrial biosphere (Sitch et al., 2015). Global terrestrial biosphere models (TBMs) have evolved during the last decades alongside our understanding of soil and vegetation functioning (Bonan and Doney, 2018). Early vegetation models included only processes related to the carbon (C) and water cycle (e.g.  Sitch et al., 2003; Krinner et al., 2005; Dickinson et al., 2006; Raddatz et al., 2007; Clark et al., 2011). The recognition that nitrogen (N) has a pivotal role in the future dynamics and C storage of terrestrial ecosystems (Vitousek and Howarth, 1991; Hungate et al., 2003) has led to the development of a new generation of models that include a comprehensive representation of the N cycle (Thornton et al., 2007; Zaehle and Friend, 2010; Gerber et al., 2010; Warlind et al., 2014). More recently, phosphorus (P) cycle processes have also been included in TBMs (Wang et al., 2010; Goll et al., 2017; Yang et al., 2014), as these can be important to understanding ecosystem response in naturally P limited tropical regions (Yang et al., 2014) or in regions with large atmospheric N deposition and ensuing increases in P limitation (Peñuelas et al., 2013; Vitousek et al., 2010).

The number of element cycles and thereby processes considered in TBMs has increased in an effort to provide more realistic models (Zaehle and Dalmonech, 2011; Prentice et al., 2015), yet there is little consensus on how to represent many of these processes in a realistic, but robust and computationally efficient manner. Often, small-scale soil and vegetation processes can lead to larger scale feedbacks (e.g. Hararuk et al., 2015; Bradford et al., 2016) and therefore need to be included in sufficient detail in terrestrial biosphere models. Recent model-data synthesis studies with observations from Free-Air $CO_2$ Enrichment (FACE) experiments have revealed a number of fundamental issues in the way that state-of-the-art models represent plant growth (De Kauwe et al., 2014), nitrogen dynamics (Zaehle et al., 2014), and water responses (De Kauwe et al., 2013) to elevated $CO_2$. This highlights the need for a modular framework that allows testing multiple hypothesis for uncertain processes, thereby gaining an understanding on how process information and importance propagates from site to regional and global scales (Knauer et al., 2016; Peng et al., 2014; Thum et al., 2017).

One important obstacle to such an approach is the gradual development of terrestrial biosphere models, which implies that new features, such as processes describing the dynamics of the N or P cycle (Gruber and Galloway, 2008; Arneth et al., 2010), have been added to existing model formulations (Bonan, 2008). This evolutionary approach can result in a situation where assumptions that were made in earlier versions of the model are incompatible with the new assumptions, or that the old model structure cannot appropriately accommodate new structures, therefore limiting the ability to take new ecophysiological understanding into account. To overcome the issues of evolutionary development, we have developed a new terrestrial biosphere model QUINCY (QUantifying Interactions between terrestrial Nutrient CYcles and the climate system, Fig. 1), benefiting from advances in the understanding of global ecology. This new model is formulated based on:

- the recognition that plant growth may be limited by source (e.g. photosynthesis) or sink (growth rate of individual tissues, constrained by nutrients, temperature, and water availability) processes (Fatichi et al., 2013). We account for this decoupling by introducing a short-term ('labile') and a long-term ('reserve') storage pool for carbon and nutrients, which allow plants to adjust the carbon partitioning between growth, respiration, and storage according to nutrient availability, moisture stress and temperature.

- the consideration of gradual changes in nutrient availability over time and their effects on the surface carbon, water, and energy exchanges. The model represents all biogeochemical and biogeophysical processes in the model at a half-hourly time-step. Many processes, e.g. the response of photosynthesis, tissue stoichiometry and fine root growth to nutrient shortage, are assumed to have a process-specific 'memory' time scale, causing a lagged response to instantaneous variations in the environmental conditions. This includes a representation of the acclimation of both photosynthesis and maintenance respiration to the prevailing growth temperature (June et al., 2004; Atkin et al., 2014; Mercado et al., 2018). Together with a dynamic representation of photosynthetic capacity based on soil nutrient availability, this feature reduces the need for regionally defined plant functional types (e.g. boreal versus temperate type) needed to describe the vegetation in different regions.

- the recognition that biogeochemical processes in the soil (e.g. soil organic matter decomposition, nitrification, denitrification, and weathering) vary strongly within the soil profile (Ahrens et al., 2015; Koven et al., 2013). Therefore, soil physics and biogeochemical processes are explicitly vertically resolved and so is the interaction between plant root uptake and turnover and soil biogeochemical processes.

We have formulated this model in a modular structure to facilitate the consistent testing of multiple hypothesis for one particular process. Additionally, we have added a number of important diagnostics, that will allow further ways of model evaluation in the future. The leaf chlorophyll content is explicitly modelled from the leaf N and used to model the light dependency of canopy photosynthesis (Kull and Kruijt, 1998), which allows for further ways to compare the simulation results with *in situ* and remotely sensed observations. The model also keeps track of the isotopic composition of C (in terms of $^{13}$C, and $^{14}$C), and N ($^{15}$N), which will allow to make use of natural abundance data and isotope tracer studies in the future.

The aim of this paper is to present the basic structure and main features of the baseline version of this new model. We provide an assessment of the model's performance against a range of observations from global-scale ecosystem monitoring networks to demonstrate that the framework is capable of consistently simulating C fluxes given the simulated N, P, and water availability across a large gradient in climate and soil conditions, as well as across different plant functional types. To aid this understanding we provide an assessment of the model's sensitivity to its parameterisation and the associated uncertainty. This information provides the background for future process-specific studies to test and improve process representation.

## 2  Methods

### 2.1  Model description

The QUINCY model v1.0 (rev. 1772) represents the coupled biogeochemical cycles of carbon (C), nitrogen (N), and phosphorus (P) in terrestrial ecosystems, as well as their interaction with the terrestrial water and energy balance (Fig. 1). The model traces the flow of these elements as well as C and N isotopes ($^{13}$C and $^{14}$C, and $^{15}$N) through vegetation and soil at a half-hourly time-step. The model considers eight broadly defined plant functional types (PFTs, see Tab. 1), representing differences in leaf type (herbaceous, broadleaved, coniferous), phenology (evergreen, rain green, and summer green), growth form (grasses and trees), and photosynthesis-type (C3 versus C4 photosynthesis) with a set of traits describing time-invariant functional differences across types (see SI Tab. 7). Different to other TBMs, certain "soft" plant functional type characteristics, such as the photosynthetic capacity of leaves or the temperature sensitivity of photosynthesis and respiration acclimate to local environmental conditions, and therefore lead to a smoother transition of ecosystem functioning across eco-climatic gradients. A brief overview of the model structure and key processes is given in this section. The detailed mathematical description of the model processes can be found in the Supplementary Material.

Although conceived to be coupled to the land-surface scheme of an Earth system model, the model is currently applied stand-alone at the ecosystem scale. The stand-alone version requires half-hourly short- and longwave radiation, air temperature, precipitation and snowfall, wind velocity, atmospheric $CO_2$, $^{13}CO_2$, $^{14}CO_2$ mole fractions, as well as rates of $NH_x$, $NO_y$, and $PO_4$ deposition as time-dependent driving data. In addition, the model requires input describing the geographical coordinates, vegetation type, and soil physical and chemical parameters (texture, bulk density, rooting and soil depth, as well as inorganic soil P content).

### 2.1.1  Vegetation processes

Vegetation is characterised by an average individual representative of a PFT, composed of three fast-lived structural tissue types (pools: leaves, fine roots, and fruits), a respiring non-structural pool (labile), as well as a seasonal, non-respiring, and non-structural storage pool (reserve). In the case of tree vegetation types, three longer-lived structural tissue types (sapwood, heartwood, and coarse roots) are additionally represented, as are stand characteristics (height, diameter, density).

Photosynthesis is calculated for sunlit and shaded leaves separately, explicitly taking the vertical canopy gradient of light, foliar chlorophyll and photosynthetic N into account (Kull and Kruijt, 1998), with extensions for C4 photosynthesis (Friend et al., 2009), and the temperature response as in Bernacchi et al. (2001, SI Sect. 2). The stomatal conductance is coupled to the calculation of photosynthesis according to the Ball-Berry formulation (Ball et al., 1987; Knauer et al., 2015). Maintenance respiration is calculated for each tissue type as a function of its N content and tissue temperature (SI Sect. 3.3, Lloyd and Taylor, 1994). Photosynthesis and respiration acclimate to growth temperature according to (Friend, 2010) and (Atkin et al., 2014), respectively. Plant nutrient uptake is dependent on fine root biomass density, soil soluble $NH_4$, $NO_3$, and $PO_4$ concentrations as well as plant internal nutrient demand (SI Sect. 4.5, Zaehle and Friend, 2010).

Different to earlier model approaches that included a labile pool (Zaehle and Friend, 2010), plant growth is modelled as the balance of source processes (photosynthesis, nutrient uptake) and the capacity of the plant to create sinks (production of new biomass tissue, respiration, and storage; SI Sect. 3.3). The capacity of the plant to generate sinks is dependent on (i) the activity of the plant's meristem controlling the usage of the labile pool for growth, which is reduced at low air temperature and/or soil moisture (Fatichi et al., 2013).; (ii) the partitioning of its labile resource to new tissue growth and the availability of nutrients to create these tissues (Zaehle and Friend, 2010); (iii) the need for longer-term storage production (Fisher et al., 2010); and (iv) respiration for maintenance, which is given priority over growth of new tissue. Short-term fluctuations in the balance between carbon acquisition through photosynthesis and nutrient acquisition by roots are balanced by the time-scale of the labile pool turnover. Seasonal and longer-term fluctuations are balanced to some extend by the build-up and use of the reserve pool. The flow of compounds between the labile and reserve pools (SI Sect. 3.6) is described by a set of pull (from the reserve pool) and push (to the reserve pool) mechanisms attempting to simulate the signalling related to the beginning of the growing season (phenological pull), the need for maintenance and growth (maintenance pull), as well as to provide resources for the next growing season or resilience against interannual variability (reserve push).

Tissue growth follows a set of allometric equations (Shinozaki et al., 1964; Sitch et al., 2003; Zaehle and Friend, 2010), describing size-dependent relationships of foliar, fine root, coarse root, sapwood and fruit biomass (SI Sect. 3.4). The allometric relationship between leaves and fine roots responds to N, P and water limitation and therefore increases uptake capacity under nutrient limitation. The C:N and N:P ratios of the leaves and fine roots are flexible within empirical bounds and respond dynamically to an imbalance between C and N, or N and P availability, respectively (SI Sect. 3.5). The allometric equations and the N and P content of each tissue give the stoichiometric constraint of plant growth. Photosynthesis can be down-regulated through sink-limitation (Hartmann et al., 2018), if nutrient or water shortage leads to the accumulation of carbon in the labile pool (SI Sect. 3.6).

Turnover is considered at two time-scales: (i) the rapid breakdown of enzymes (N) and associated RNA (P) from tissue, and their ensuing replacement from the labile N and P pools (recycling; at the time scale of days, Zaehle and Friend, 2010); and (ii) the senescence of entire tissues and their conversion to litter, including the resorption of nutrients from foliage (SI Sect. 3.9). Tissue senescence is calculated given a fixed turnover time for each tissue, with the exception of the leaves, where turnover is determined by the PFT-specific phenological timing (SI Sect. 3.8).

Stand-level vegetation dynamics are represented through density-dependent mortality, as well as a dynamic background mortality related to the overall growth efficiency of the plant (Sitch et al., 2003; Zaehle and Friend, 2010, SI Sect. 3.10). Re-establishment/Recruitment is explicitly taking account of the available seed pool at the forest / grassland floor, thereby depending amongst others on the vegetation's ability to produce fruit.

### 2.1.2 Soil biogeochemical processes

The vertical soil profile of biogeochemical pools and processes is explicitly represented, with exponentially increasing layer thickness with increasing soil depth. For each of these layers, the model represents different organic pools (metabolic, structural, and woody litter, as well as fast and slow overturning soil organic matter (SOM)), as well as inorganic pools of N and

P (soluble inorganic $NH_4$, $NO_3$, as well as $NO_y$, $N_2O$, and $N_2$, soluble inorganic $PO_4$, adsorbed $PO_4$, occluded $PO_4$ and primary $PO_4$). For each soil layer, temperature and moisture are calculated based on soil physical characteristics, and the transport and atmospheric exchange of energy and water (SI Sect. 6.3).

The turnover and formation of SOM follows, with some modifications, the CENTURY approach (Parton et al., 1993, SI-
Sect. 4): the turnover of litter and SOM pools are all calculated using first-order kinetics with temperature and moisture dependence. The litter stoichiometry is determined by the stoichiometry of senescent plant tissue and tissue-specific allocation fractions. The stoichiometry of the fast SOM pool adjusts to available inorganic nutrients, whereas the slow SOM pool is assumed to have fixed C:N:P stoichiometry.

The soluble inorganic $NH_4$, $NO_3$ and $PO_4$ are assumed to be available for plant and microbial uptake, as concluded by White
(2006) and many others. Plants and soil microbes compete for these nutrients based on their respective demand and uptake capacity, which varies in time and with soil depth. In the aerobic part of the soil, $NH_4$ is oxidised to $NO_3$ through nitrification and in the anaerobic part of the soil $NO_3$ is reduced to $N_2$ through denitrification (Zaehle et al., 2011). Both processes produce $NO_y$ and $N_2O$ as by-products (SI Sect. 4.7). The representation of soil inorganic P dynamics (SI Sect. 4.8) follows the concept from Yang et al. (2014) and Wang et al. (2010). The available soluable $PO_4$ is exchanged via ad-/desorption with the mineral
surface, leached with soil water, and replenished by atmospheric deposition, weathering, and biomineralisation of P that is bound in the slow SOM pool. The adsorbed P is further absorbed into the soil matrix and gradually becomes an inactive form of P (occluded P, Walker and Syers, 1976).

## 2.2 Data for model evaluation

We evaluate simulated diurnal and seasonal patterns of gross primary production and net ecosystem carbon exchange (GPP and
NEE, respectively) at a subset of FLUXNET sites (see Table A1) available from the FLUXNET La Thuile Synthesis Dataset (NOA, 2007). The half-hourly $CO_2$ fluxes have been measured and processed using standard procedures (Papale et al., 2006) as well as gap-filling and partitioning algorithms (Reichstein et al., 2005). We further evaluate the mean annual estimates of gross and net primary production (GPP and NPP, respectively) and their ratio, the carbon-use efficiency (CUE = NPP / GPP) from a global forest database (GFDB, Vicca et al., 2012; Campioli et al., 2015). We further evaluate the simulated growing-season
plant water-use efficiency, i.e. the ratio of plant water loss to carbon uptake, by comparing a proxy, foliar isotope discrimination of $^{13}C$ (Medlyn et al., 2017), against data reported by (Cornwell et al., 2018a, b). Fig. 2 provides an overview of the sites used for evaluation.

## 2.3 Model setup

### 2.3.1 Boundary conditions and meteorological forcing

The QUINCY model is applied at site scale for the dominant plant functional type (PFT) at each site. For the simulations at the FLUXNET sites, the site-specific observed meteorological data were used (NOA, 2007). For the GFDB sites, where site-level meteorology is not readily available, daily meteorological data for 1901 to 2015 was taken from CRUNCEP, version 7, (Viovy,

2016), and disaggregated to the model time-step using the statistical weather generator as in Zaehle and Friend (2010). The annually changing $CO_2$ mole fraction was obtained from Le Quéré et al. (2018), and the time series of $^{13}C$, $^{14}C$ are obtained from Graven et al. (2017). The time series of N deposition for each site is taken from Lamarque et al. (2010) and Lamarque et al. (2011). For the P deposition model, estimates of nutrient and dust fluxes from Brahney et al. (2015); Chien et al. (2016) were used.

Soil physical properties (volumetric heat capacity and conductivity, water content at saturation, field capacity, and wilting points, as well as parameters describing the soil water retention curve are derived from soil texture according to Saxton and Rawls (2006). Where available, texture data are taken from site observations. Alternatively, they are obtained from the nearest gridcell of the SoilGrids dataset (Hengl et al., 2017).

The vegetation is initialised as bare ground with a small amount of seed-bed mass to start vegetation growth. The soil organic matter profile is initialised with a default SOM content for each pool, 60% of which is allocated to the uppermost layer, and the remaining 40% is allocated to other soil layers in proportion to the assumed rooting profile. Previous tests have shown that the model is not very sensitive to the choice of the SOM initial condition. The soil inorganic P pools of the first 50 cm are initialised using the soil P dataset by Yang et al. (2013), extrapolated to the whole soil profile assuming i) a constant total soil inorganic P density (mol P kg$^{-1}$ soil), and ii) an increasing fraction of primary P and decreasing fraction of labile P with increasing soil depth.

### 2.3.2 Spinup and model protocol

The QUINCY model is spun-up with repeated meteorological forcing for each site to obtain an near-equilibrium soil and vegetation state. For the GFBD sites, meteorology and other atmospheric forcing (atmospheric $CO_2$, its isotopes, as well as N and P deposition), are taken by randomly drawing years from the period 1901 to 1930. The same procedure is applied for FLUXNET sites, with the exception that meteorological forcing is only available for more recent years, and data from those years are used in random sequence. The P cycle is activated during the model spinup, but the more stable soil inorganic P pools, i.e. the primary, sorbed, occluded pools, are kept constant to ensure that the simulation initialises at the P status of Yang et al. (2013)'s dataset.

After spinup, the model is run for the period 1901-2015 using the annual values for atmospheric $CO_2$, $^{13}CO_2$ and $^{14}CO_2$, as well as N and P deposition, and the meteorology of the respective year. For the comparison to GFDB data, forest stands are clear-cut in the year provided by the database. Upon harvest, vegetation biomass is transferred to the litter pools, with the exception of the wood pool, of which a given fraction, $f_{harvest}^{wood}$, is removed from the site. In the case of FLUXNET sites, we retain the model output for the years covered by the available data at each individual site (Tab. A1). For the GFDB sites, we average over the period 1995-2004 to remove the effects of interannual climate variability and to have modelled forest age close to the actual forest age of each site, as the precise year of measurement is not recorded in the database for all sites.

To test the effect of the simulated N and P availability, we applied the model for the FLUXNET sites with three different setups. Next to the full CNP version of the model described above (referred to hereafter as 'CNP'), we performed a simulation ('CN') in which the P concentration of the soil was kept at concentrations not limiting microbial or plant uptake, effectively

removing the impact of the inorganic P sorption and weathering dynamics, and maintaining N:P stoichiometry at default values. We also added a version ('C'), in which in addition, biological N fixation in soil (asymbiotic fixation) and in vegetation (symbiotic fixation) was calculated so as to avoid any N limitation of soil turnover and vegetation growth while keeping the C:N stoichiometry at default values.

## 2.4 Model sensitivity to its parameterisation

We further test the sensitivity of the model to its parameterisation using a hierarchical latin hypercube design (LHS, Saltelli et al., 2000; Zaehle et al., 2005). As many parameters have unknown value ranges and distributions, we simply vary each parameter between 90% to 110% of its default value given in the Supplementary Material, drawn with LHS sampling from a uniform distribution. We first generate LHS samples for each module (corresponding to one Section in the SI, *results not shown*), and evaluate the model output from these simulations in terms of long-term mean modelled GPP, leaf C:N:P, net N and P mineralisation, as well as total vegetation and ecosystem carbon storage. Based on these simulations we select parameters (n=45), which have a strong effect on the model outcome to form a new set of 1000 LHS samples, which are used for the model sensitivity and uncertainty analysis presented in this paper. We measure parameter importance as the rank-transformed partial correlation coefficient (RPCC) to take account of potential non-linearities in the relationship between parameters and model output (Saltelli et al., 2000; Zaehle et al., 2005).

## 3 Results

### 3.1 Simulated diurnal to seasonal time-scale carbon dioxide fluxes at selected FLUXNET sites

We first compare the simulated mean monthly diurnal, as well as the mean seasonal cycle of gross primary production (GPP) at four forest sites, representing the major tree plant functional types, with *in situ* observations (Fig. 3). The model simulations agree reasonably well with the observations in that the general diurnal and seasonal timing and overall magnitude of fluxes are consistent. Importantly, while the N and P cycles dampen the overall magnitude of the fluxes at the beech forest site (temperate broad-leaved deciduous; FR-Hes) and the eucalyptus forest site (temperate broad-leaved evergreen; AU-Tum), they do not affect the shape of either the diurnal or seasonal cycles. In other words, the diurnal and seasonal changes in nutrient availability only affect the long-term, but not the short-term vegetation gross carbon uptake. There is little overall effect of the nutrient cycles on the correlation between half-hourly simulated and observed GPP at FI-Hyy ($r^2$=0.76), FR-Hes ($r^2$=0.63), and BR-Ma2 ($r^2$=0.67), and only a minor reduction for AU-Tum ($r^2$ 0.70 versus 0.65 for C and CN(P), respectively). The largest decrease of the model's root mean square error (RMSE) took place at FR-Hes, where introducing N and P cycling reduced the RMSE by nearly 20% to 5.17 $\mu$molm$^{-2}$s$^{-1}$. For FI-Hyy the RMSE and the improvement were 2.42 and 0.11 $\mu$molm$^{-2}$s$^{-1}$. For AU-Tum the RMSE and worsening of RMSE were 5.44 and 0.36 $\mu$molm$^{-2}$s$^{-1}$. At BR-Ma2 the RMSE and the improvement were 7.78 and 0.09 $\mu$molm$^{-2}$s$^{-1}$. At the tropical evergreen forest site BR-Ma2 (Fig. 3d, f) the different versions performed similarly. The lower GPP in the daily observation-based estimate between day of year 150 and 200, which

Geoscientific Model Development
10.5194/gmd-2019-49
2019-04-01
journal article
en

are not replicated by the model, are largely caused by lower observation-based GPP at the start of the time-series during this time of year in 2003. There was no obvious cause for this behaviour visible in the meteorological drivers.

Table 2 summarises the key C, N and P stocks and fluxes simulated with the CNP version of the model for these four FLUXNET sites, calculated for the time period of the flux observations (Table A1). The annual GPP from the $CO_2$ flux observations is in line with the modelled values for FI-Hyy (observed 1016 $gCm^{-2}yr^{-1}$), and FR-Hes (observed 1874 $gCm^{-2}yr^{-1}$), while productivity at BR-Ma2 (observed: 2557 $gCm^{-2}yr^{-1}$) is somewhat overestimated, and strongly underestimated at AU-Tum (observed: AU-Tum: 2151 $gCm^{-2}yr^{-1}$). Simulated foliar C:N was within the observational range reported in the La Thuille database (NOA, 2007) for all four sites (observed: 41, 21, 35 and 20-35, for FI-Hyy, FR-Hes, AU-Tum and BR-Ma2, respectively). Nutrient availability and fluxes are not consistently available for these sites.

The Taylor plots of the half-hourly simulated and observation-based time-series of GPP and NEE (Fig. 4) demonstrate that the overall model performance noted in Fig. 3 holds across a wider set of sites, spanning a larger climatic gradient and also including grassland sites. The Taylor plot reports results obtained with the CNP version of the model; the plots for the C and CN version were very similar in terms of their correlation and moderately different in terms of the ratio of standard deviations. The simulated GPP shows slightly better performance over the different sites than NEE. Considering that i) the model has not been parameterised specifically for each site and ii) eddy-covariance observations at this time-scale are subject to considerable fluctuations, the model performance is acceptable in terms of the correlation. While there is a wide spread in the ratio of the simulated to observation-based standard deviation, mostly associated with site-based differences in the seasonal maximum of the flux, there is no systematic model bias for any PFT.

The inclusion of the N cycle (difference between C and CN model versions) reduces the root mean squared error (RMSE) between simulated and observation-based estimates of GPP for all PFTs apart from the tropical broad-leaved evergreen PFT (Fig. 5). The largest reductions of the RMSE between the different versions occurs for TeBE (34.0 %) and TeH (41.6 %). There is no strong effect of including the P cycle on simulated GPP, and in consequence there is no difference in the RMSE values of the CN and CNP versions, even for the tropical broad-leaved evergreen forest sites, which are in regions typically associated with P-limitation of biomass production.

## 3.2 Cross-site analysis of long-term mean GPP and NPP

Simulated GPP across all the GFDB sites (n=434), covering a range of tree PFTs, agrees reasonably well with data ($r^2 = 0.55$, RMSE=560 $gCm^{-2}yr^{-1}$) (Fig. 6a), despite an underestimation of GPP for some sites, both in tropical forest ecosystems and needle-leaved evergreen forests. The data shown are restricted to forests older than 20 years, to avoid ambiguities in the model-data comparison as the exact method of forest regeneration after disturbance is not known and the model does not describe stand-level dynamics of very early succession forests that often have very high observed productivity. The model is also able to replicate the observations from low to modest NPP values albeit with a higher relative RMSE (Fig. 6b) ($r^2 = 0.35$, RMSE=305 $gCm^{-2}yr^{-1}$). While there is no systematic over- or underestimation of NPP with PFT or magnitude of NPP, it is noteworthy that the highest NPP value simulated for this dataset was only 1441 $gCm^{-2}yr^{-1}$, whereas for a few sites, observation-based estimates reached nearly 2000 $gCm^{-2}yr^{-1}$. The model correctly predicts the range of carbon-use efficiency (CUE), i.e. the

ratio of net to gross primary production, where the observed CUE values ranged between 0.21 and 0.76 g g$^{-1}$, while the simulated values were between 0.19 and 0.61 g g$^{-1}$. The model also predicts correctly a lower CUE in tropical compared to temperate/boreal ecosystems. However, the model is not able to explain the within PFT-variability of the observed CUE values in the dataset (Fig. 6c).

5    The discrimination of leaf $\Delta^{13}$C against an index of water availability (evapotranspiration divided by the potential evapotranspiration) (ET/PET) from observations (Cornwell et al., 2018b) and the GFDB simulations are shown in Fig. 7. Both observations and model showed less discrimination of $\Delta^{13}$C in drier conditions, indicating an effect of seasonal water availability in overall drought stress on photosynthesis. Comparing PFT-wise mean values, constrained to estimates of ET/PET > 0.25 to remove the effect of modelled outliers under high water-limitation, the average for broadleaf deciduous forest (BS) was

10    20.88 ‰ for the observations and 20.67 ‰ for the modelled values. For the needle-leaved deciduous (NS) PFT the average values were very similar (observations 20.29 ‰ and simulations 20.12 ‰). Somewhat larger discrepancies occurred for the needle-leaved evergreen PFT, where the average of the observations was 20.00 ‰ and the average of the simulation results was 19.59 ‰. For the broadleaf evergreen forests there was a large deviation between the observed (22.68 ‰) and modelled values (20.55 ‰), but also the sample sizes were very different (n=1617 for observations and n=54 for simulations). For the modelled

15    values the difference between needle-leaved deciduous and evergreen forests was more pronounced than in the observations, but the sample size of modelled NS sites was very small (n=6).

### 3.3   Model sensitivity and uncertainty analysis

The parameter sensitivity study reveals that the inner-quartile range of the model output (Fig. 8) is well constrained and centred around the results of the standard parameterisation reported in Tab. 2. Extreme parameter combinations cause larger variations,

20    but do not fundamentally change the model behaviour. By varying parameters, we essentially generate an ensemble of simulations with different soil nutrient retention capacities and turnover rates, as well as vegetation nutrient-use efficiencies, thus a gradient of sites with identical climate, but different N and P availabilities. The model shows, as expected, clear dependencies between the rates of net N and P mineralisation, GPP, and carbon stock in vegetation and soil. The correlation between foliar C:N:P and biogeochemical fluxes is less clear, owing to the additional effects of productivity changes on foliar area and carbon

25    partitioning belowground.

The role of specific parameters varies with the output quantity of interest and across sites, depending on the level of nutrient limitation at the sites. Table Tab. 3 lists the ten most important parameters for each site, clearly demonstrating that next to parameters affecting leaf mass and photosynthetic efficiency directly (e.g. $k_0^{struc}$, $sla$, $a_{chl}^n$, $k_{latosa}$), the assumed overall turnover time of the soil, affected through the optimum temperature of decomposition, $T_{opt,decomp}$, as well as the efficiencies

30    of microbial SOM processing ($\eta_{C,litter \rightarrow fast}$, $\eta_{C,fast \rightarrow slow}$) play an important role due to the strong coupling of vegetation productivity to soil nutrient availability in the QUINCY v1.0 model.

## 4 Discussion

Models of coupled carbon-nitrogen and phosphorus cycles for land surface models have been published before (Goll et al., 2017; Wang et al., 2010; Yang et al., 2014). The QUINCY v1.0 model introduced in this paper distinguishes itself from these models in that it seamlessly integrates nutrient dynamics with carbon, water and energy calculations (e.g. there is no difference

5  in time-stepping between biogeophysical and biogeochemical processes) and that there is an explicit consideration of the decoupling of photosynthesis and growth as opposed to the simpler treatment of these dynamics in Zaehle and Friend (2010), as applied in Goll et al. (2017). The purpose of this paper is to provide a background for future studies on the effect of coupled biogeochemical cycles at large scales as well as on testing the effect alternative representations of important nutrient cycle related processes, for which the model is suitable due to its modular design. A detailed evaluation of all new submodules of

10  the model is beyond the scope of this paper.

    Overall, QUINCY v1.0 performs well in terms of diurnal, seasonal and annual carbon fluxes across a range of ecosystem monitoring flux sites, spanning a large geographic gradient and a variety of ecosystem types. Despite the lack of any site-specific parameterisation, there is no systematic model bias for any single PFT at either time-scale. Including a coupling of the carbon cycle to representations of the nitrogen and phosphorus cycle affects long-term productivity through its effects

15  on photosynthetic capacity (changed foliar nitrogen concentration) and leaf area (as a result of the changes in root:shoot allocation), but diurnal and seasonal variations in nitrogen or phosphorus availability do not affect simulated productivity because of the buffering introduced through the labile and reserve storage.

    Model predictions generally show an improvement in the prediction of GPP with the addition of the N cycle. This occurs despite a slight low bias in simulated foliar nitrogen concentration compared to the mean values of the TRY database (BS: 2.1

20  (0.6-3.2) % versus $1.7 \pm 0.3$, TrBE/TeBE: 1.7 (0.5-3.9) % versus $1.7 \pm$, NE: 1.3 (0.5-1.9) % versus $1.0 \pm 0.4$, NS: 1.9 (0.9-3.0) % versus $1.8 \pm 0.2$ observed and simulated, respectively Kattge et al., 2011). This comparison is indicative only, since there is a geographic mismatch between the spatial coverage and distribution of the modelled sites and the data in the TRY database. Note that these estimates are not fully independent because the minimum and maximum range of permissable foliar N were derived from (Kattge et al., 2011).

25     The P enabled version does not show additional improvement in simulating the regional differences in productivity. This is partly due to the fact that the sites with sufficient information on GPP and NPP available for model evaluation are as a majority located in temperate and boreal regions, where the main limiting nutrient is likely to be nitrogen (LeBauer and Treseder, 2008). However, even for the few tropical sites included in the analysis, where in general terms limitation of productivity by P would be expected (LeBauer and Treseder, 2008; Vitousek et al., 2010), we do not find any significant effect of the simulated P

30  cycle. An important contributor is the fact that in QUINCY v1.0, the vertically explicit description of SOM dynamics permits very efficient recycling of organic P in the litter layer, where low mineral sorption capacities lead to efficient P uptake of soil microorganisms and vegetation. The efficient recycling in the litter layer is partially due to the biochemical mineralisation flux. Further observations are required in order to constrain this flux better (Reed et al., 2011). One further important factor is the unknown initial soil concentration of plant available P, as well as uncertainties in the rate of P weathering. Improving

the understanding of P availability across the globe remains an important challenge for the representation of P effects on productivity (Wang et al., 2010; Goll et al., 2017), requiring detailed observations of soil and vegetation P dynamics and manipulation experiments (e.g. Medlyn et al., 2016). In addition, similar to other models (Goll et al., 2017; Yang et al., 2014), QUINCY v1.0 currently assumes that P limitation solely effects productivity due to a stoichiometric constraint on growth,

5 while other mechanisms may also play an important role in the acclimation of plant processes to different levels of P availability (Jiang et al., 2019).

The predicted GPP and NPP across a large range of climatic and biogeographic situations is in good agreement with observations, and so is the average of the carbon-use efficiency (CUE = NPP/GPP). However, the model does not reproduce the observed range in CUE in temperate and boreal forests. Vicca et al. (2012) suggested that this variance is associated with altered

10 carbon partitioning, and in particular increased belowground carbon allocation in response to nutrient shortage. This inference is consistent with detailed observations at the FLUXNET site FI-Hyy (Ilvesniemi et al., 2009; Korhonen et al., 2013), where the QUINCY v1.0 model successfully simulated GPP, and vegetation C storage (observed 6.80 $\mathrm{kgCm}^{-2}$, (Ilvesniemi et al., 2009)), but substantially overestimated the NPP (observed: 242 $\mathrm{gCm}^{-2}\mathrm{yr}^{-1}$). Additionally, the N uptake by the vegetation in addition to the N losses were in the same order of magnitude as the observations (Korhonen et al., 2013), suggesting that

15 C partitioning rather than N availability is the source of the underestimation. The QUINCY v1.0 model simulates an increase of the root:shoot ratio with response to nutrient stress. However, the effect of this change on CUE is small, as increased root allocation not only decreases biomass production through increased allocation to higher turnover tissue, but also whole-plant mass-specific respiration, given the implicit model assumption that mass-specific fine root respiration is smaller than leaf-mass specific respiration. Further causes of this model-data mismatch include alternative pathways of carbon partitioning not repre-

20 sented in the model (e.g. exudation), changes in tissue turnover times with changes in nutrient availability, and the magnitude of mass-specific autotrophic respiration. For instance, the estimated autotrophic respiration in FI-Hyy was 714 $\mathrm{gCm}^{-2}\mathrm{yr}^{-1}$ (Ilvesniemi et al., 2009), compared to 486 in the model $\mathrm{gCm}^{-2}\mathrm{yr}^{-1}$, which may be the combined result of allocation, temperature response and specific respiration rates, particularly below ground. The novel structure of the QUINCY v1.0 model that decouples photosynthesis from growth, and therefore permits to adjust carbon partitioning to different sinks at short timescales

25 will allow to investigate the effect of these processes in the future.

The comparison of simulated leaf $^{13}\mathrm{C}$ discrimination to observations recorded in the global dataset by (Cornwell et al., 2018b) suggests that the overall parameterisation of long-term mean leaf- and ecosystem-level water-use efficiency, derived from instantaneous leaf-level gas exchange measurements (Lin et al., 2015), broadly conforms with observations. Notably, the model also simulates the trend in discrimination with respect to changing water availability in accordance with observations,

30 which suggests that the overall effect of moisture availability on water-use efficiency is appropriately considered by the model. Discrepancies between the observation-based estimates of water-use efficiency derived from leaf-level flux and isotope measurements have been noted before (Medlyn et al., 2017), and these may contribute to the remaining model-data mismatch. One possible reason for this mismatch may be the omission of mesophyll conductance in model formulations, which may induce systematic shifts in chloroplast $[\mathrm{CO_2}]$, and thereby affect the simulated value of leaf $\Delta^{13}\mathrm{C}$ without affecting leaf-level

35 water-use efficiency (Knauer et al., in press).

## 5  Summary and future directions

In this paper, we presented the mathematical formulation of a new terrestrial biosphere model, QUINCY v1.0, that includes a number of ecophysiological processes (short-term and long-term storage pools, acclimation processes) that have not been represented in earlier TBMs. We evaluated QUINCY v1.0 against a range of observations from worldwide datasets and demonstrated

5   that it is successful in simulating photosynthesis and plant dynamics across large geographical ranges and different ecosystem types with different levels of chronic nutrient input and water availability. We further demonstrated that despite increased complexity and therefore increased numbers of weakly constrained parameters, the model produces predictions of the coupled biogeochemical cycles at site level within reasonable and well-defined bounds. The model evaluation provided in this paper points to shortcomings of the baseline QUINCY model in terms of the responses of carbon partitioning to nutrient availability,

10   and the interactions between plants and soil processes.

The next logical step in the model's evaluation is to subject it to a range of manipulative experimental settings that will test the realism of the coupling of the carbon-nitrogen-phosphorus cycle in different climate regimes (Zaehle et al., 2014; Yang et al., 2014; Medlyn et al., 2015). Such model evaluation can help point to the adequate representation of individual processes rather than just overall model performance. The inclusion of isotope tracers will increase the scope of such comparisons, since

15   this will allow to better track carbon and nitrogen flows.

One of the motivations behind the development of the QUINCY v1.0 model was the recognition that there may be more than one adequate model representation for one process (Beven, 2008). Therefore the model has been constructed with a modular design, allowing to replace some of its components by alternative representations to test their effect on model predictions. Examples of future work with QUINCY v1.0 include the control of plants to shape carbon, nitrogen and phosphorus partitioning

20   and thereby plant functioning in response to environmental change, and plant-soil processes by including better representations of the interactions between root growth/activity and SOM turnover and stabilisation.

These basic benchmarks provide a baseline test to integrate QUINCY v1.0 into the JSBACH land surface model (Mauritsen et al., 2019) to allow for a spatially explicit simulation, and integration of a range of important processes such as fire disturbance, land-use and permafrost dynamics. In the mid-term, this will allow coupling to the Max Planck Institute's Earth

25   System Model (MPI-ESM) framework ICON to address feedbacks between land biogeochemistry and climate on the basis of an improved representation of biological processes affecting land biogeochemical and biogeophysical processes.

*Code availability.* The scientific code of QUINCY requires software from the MPI-ESM environment, which is subject to the MPI-M-Software-License-Agreement in its most recent form (http://www.mpimet.mpg.de/en/science/models/license). The source code is available online, but its access is restricted to registered users and the fair-use policy stated on https://www.bgc-jena.mpg.de/bgi/index.php/Projects/

30   QUINCYModel. Readers interested in running the model should contact the corresponding authors for a username and password.

## Appendix A:  FLUXNET sites

**Table A1.** FLUXNET sites

| Site | Long | Lat | PFT | Start | End | Reference |
|---|---|---|---|---|---|---|
| AT-Neu | 11.32 | 47.12 | TeH | 2002 | 2005 | Wohlfahrt et al. (2008b) |
| AU-How | 131.15 | -12.49 | TeBE | 2002 | 2005 | Beringer et al. (2011) |
| AU-Tum | 148.15 | -35.66 | TeBE | 2002 | 2005 | Cleugh et al. (2007) |
| BE-Bra | 4.52 | 51.31 | TeNE | 2000 | 2002 | Carrara et al. (2004) |
| BR-Ma2 | -60.21 | -2.61 | TrBE | 2003 | 2005 | Araújo et al. (2002) |
| CA-Man | -98.48 | 55.88 | BNE | 1999 | 2003 | Dunn et al. (2007) |
| CA-Qfo | -74.34 | 49.69 | BNE | 2004 | 2006 | Bergeron et al. (2007) |
| CA-SF1 | -105.82 | 54.49 | BNE | 2004 | 2005 | Mkhabela et al. (2009) |
| CH-Oe1 | 7.73 | 47.29 | TeH | 2002 | 2006 | Ammann et al. (2007) |
| DE-Bay | 11.87 | 50.14 | TeNE | 1997 | 1998 | Rebmann et al. (2004) |
| DE-Hai | 10.45 | 51.08 | TeBS | 2000 | 2006 | Kutsch et al. (2008) |
| DE-Meh | 10.66 | 51.28 | TeH | 2004 | 2006 | Scherer-Lorenzen et al. (2007) |
| DE-Tha | 13.57 | 50.96 | TeNE | 1998 | 2003 | Grünwald and Bernhofer (2007) |
| DK-Sor | 11.65 | 55.49 | TeBS | 1997 | 2006 | Lagergren et al. (2008) |
| ES-ES1 | -0.32 | 39.35 | TeNE | 1999 | 2004 | Sanz et al. (2004) |
| ES-LMa | -5.77 | 39.94 | TrH | 2004 | 2006 | Vargas et al. (2013) |
| FI-Hyy | 24.29 | 61.85 | BNE | 2001 | 2006 | Suni et al. (2003) |
| FR-Hes | 7.06 | 48.67 | TeBS | 2001 | 2006 | Granier et al. (2000) |
| FR-LBr | -0.77 | 44.72 | TeNE | 2003 | 2006 | Berbigier et al. (2001) |
| FR-Pue | 3.60 | 43.74 | TeBE | 2001 | 2006 | Keenan et al. (2010) |
| IL-Yat | 34.90 | 31.35 | TeNE | 2001 | 2002 | Grünzweig et al. (2003) |
| IT-Cpz | 12.38 | 41.71 | TeBE | 2001 | 2006 | Tirone et al. (2003) |
| IT-MBo | 11.05 | 46.02 | TeH | 2003 | 2006 | Wohlfahrt et al. (2008a) |
| IT-Ro2 | 11.92 | 42.39 | TeBS | 2002 | 2006 | Tedeschi et al. (2006) |
| IT-SRo | 10.28 | 43.73 | TeNE | 2003 | 2006 | Chiesi et al. (2005) |
| NL-Loo | 5.74 | 52.17 | TeNE | 1997 | 2006 | Dolman et al. (2002) |

**Table A1.** FLUXNET sites (continued)

| Site | Long | Lat | PFT | Start | End | Reference |
|------|------|-----|-----|-------|-----|-----------|
| SE-Fla | 19.46 | 64.11 | BNE | 2000 | 2002 | Lindroth et al. (2008) |
| SE-Nor | 17.48 | 60.09 | BNE | 1996 | 1997 | Lagergren et al. (2008) |
| US-Blo | -120.63 | 38.90 | TeNE | 2000 | 2006 | Goldstein et al. (2000) |
| US-Ha1 | -72.17 | 42.54 | TeBS | 1995 | 1999 | Urbanski et al. (2007) |
| US-Ho1 | -68.74 | 45.20 | TeNE | 1996 | 2004 | Hollinger et al. (1999) |
| US-MMS | -86.41 | 39.32 | TeBS | 2000 | 2005 | Schmid et al. (2000) |
| US-MOz | -92.20 | 38.74 | TeBS | 2005 | 2006 | Gu et al. (2006) |
| US-SRM | -110.87 | 31.82 | TeBE | 2004 | 2006 | Scott et al. (2009) |
| US-Syv | -89.35 | 46.242 | TeNE | 2002 | 2004 | Desai et al. (2005) |
| US-Ton | -120.97 | 38.43 | TeBE | 2002 | 2006 | Ma et al. (2007) |
| US-Var | -120.95 | 38.41 | TrH | 2001 | 2006 | Ma et al. (2007) |
| US-WCr | -90.08 | 45.81 | TeBS | 2000 | 2005 | Cook et al. (2004) |
| VU-Coc | 167.19 | -15.44 | TrBE | 2002 | 2003 | Roupsard et al. (2006) |
| ZA-Kru | 31.50 | -25.02 | TrBR | 2001 | 2003 | Archibald et al. (2010) |

*Author contributions.* SZ conceived the model. TT, SC, LY, MK, and SZ developed the model. JE helped with model implementation and testing. All authors contributed to the interpretation of the results and writing of the manuscript.

*Competing interests.* The authors declare that there are no competing interests

*Acknowledgements.* This work was supported by the European Research Council (ERC) under the European Union's Horizon 2020 research
5 and innovation programme (QUINCY; grant no. 647204). LY was supported by the framework of Priority Program SPP 1685 "Ecosystem Nutrition: Forest Strategies for Limited Phosphorus Resources" of the German Research Foundation (DFG), grant No.ZA 763/2-1. We are grateful to Steffen Richter for technical assistance in developing the code, as well as to Sara Vicca for providing access to the GFDB data base. This work used eddy covariance data acquired by the FLUXNET community and in particular by the following networks: AmeriFlux (US Department of Energy, Biological and Environmental Research, Terrestrial Carbon Program (DE-FG02-04ER63917 and DE-FG02-
10 04ER63911)), AfriFlux, AsiaFlux, CarboAfrica, CarboEuropeIP, CarboItaly, CarboMont, ChinaFlux, FluxnetCanada (supported by CFCAS, NSERC, BIOCAP, Environment Canada, and NRCan), GreenGrass, KoFlux, LBA, NECC, OzFlux, TCOS-Siberia, and USCCC. We acknowledge the financial support to the eddy covariance data harmonization provided by CarboEuropeIP, FAO-GTOS-TCO, iLEAPS, the Max Planck Institute for Biogeochemistry, the National Science Foundation, the University of Tuscia, Université Laval and Environment Canada, and the US Department of Energy and the database development and technical support from Berkeley Water Center, Lawrence
15 Berkeley National Laboratory, Microsoft Research eScience, Oak Ridge National Laboratory, the University of California-Berkeley, and the University of Virginia.

# References

Ahrens, B., Braakhekke, M. C., Guggenberger, G., Schrumpf, M., and Reichstein, M.: Contribution of sorption, DOC transport and microbial interactions to the 14C age of a soil organic carbon profile: Insights from a calibrated process model, Soil Biology and Biochemistry, 88, 390–402, 2015.

5  Ammann, C., Flechard, C., Leifeld, J., Neftel, A., and Fuhrer, J.: The carbon budget of newly established temperate grassland depends on management intensity, Agriculture, Ecosystems & Environment, 121, 5 – 20, https://doi.org/https://doi.org/10.1016/j.agee.2006.12.002, http://www.sciencedirect.com/science/article/pii/S0167880906004300, the Greenhouse Gas Balance of Grasslands in Europe, 2007.

Araújo, A. C., Nobre, A. D., Kruijt, B., Elbers, J. A., Dallarosa, R., Stefani, P., von Randow, C., Manzi, A. O., Culf, A. D., Gash, J. H. C., Valentini, R., and Kabat, P.: Comparative measurements of carbon dioxide fluxes from two nearby towers in a cen-

10  tral Amazonian rainforest: The Manaus LBA site, Journal of Geophysical Research: Atmospheres, 107, LBA 58–1–LBA 58–20, https://doi.org/10.1029/2001JD000676, https://agupubs.onlinelibrary.wiley.com/doi/abs/10.1029/2001JD000676, 2002.

Archibald, S., Nickless, A., Govender, N., Scholes, R. J., and Lehsten, V.: Climate and the inter-annual variability of fire in southern Africa: a meta-analysis using long-term field data and satellite-derived burnt area data, Global Ecology and Biogeography, 19, 794–809, https://doi.org/10.1111/j.1466-8238.2010.00568.x, https://onlinelibrary.wiley.com/doi/abs/10.1111/j.1466-8238.2010.00568.x, 2010.

15  Arneth, A., Harrison, S. P., Zaehle, S., Tsigaridis, K., Menon, S., Bartlein, P. J., Feichter, J., Korhola, A., Kulmala, M., O'Donnell, D., Schurgers, G., Sorvari, S., and Vesala, T.: Terrestrial biogeochemical feedbacks in the climate system, Nat. Geosci., 3, 525, 2010.

Atkin, O. K., Meir, P., and Turnbull, M. H.: Improving representation of leaf respiration in large-scale predictive climate–vegetation models, New Phytologist, 202, 743–748, https://doi.org/10.1111/nph.12686, https://nph.onlinelibrary.wiley.com/doi/abs/10.1111/nph.12686, 2014.

20  Ball, J., Wooddrow, I., and Berry, J. A.: A model predicting stomatal conductance and its contribution to the control of photosynthesis under different environmental conditions, in: Progress in Photosynthesis Research, edited by Biggens, J., pp. 1–4, Dordrecht, The Netherlands, 1987.

Berbigier, P., Bonnefond, J.-M., and Mellmann, P.: CO2 and water vapour fluxes for 2 years above Euroflux forest site, Agricultural and Forest Meteorology, 108, 183 – 197, https://doi.org/https://doi.org/10.1016/S0168-1923(01)00240-4, http://www.sciencedirect.com/science/

25  article/pii/S0168192301002404, 2001.

Bergeron, O., Margolis, H. A., Black, T. A., Coursolle, C., Dunn, A. L., Barr, A. G., and Wofsy, S. C.: Comparison of carbon dioxide fluxes over three boreal black spruce forests in Canada, Global Change Biology, 13, 89–107, https://doi.org/10.1111/j.1365-2486.2006.01281.x, https://onlinelibrary.wiley.com/doi/abs/10.1111/j.1365-2486.2006.01281.x, 2007.

Beringer, J., Hutley, L. B., Hacker, J. M., Neininger, B., and U, K. T. P.: Patterns and processes of carbon, wa-

30  ter and energy cycles across northern Australian landscapes: From point to region, Agricultural and Forest Meteorology, 151, 1409 – 1416, https://doi.org/https://doi.org/10.1016/j.agrformet.2011.05.003, http://www.sciencedirect.com/science/article/pii/S016819231100147X, savanna Patterns of Energy and Carbon Integrated Across the Landscape (SPECIAL), 2011.

Bernacchi, C. J., Singsaas, E. L., Pimentel, C., Protis JR, A. R., and Long, S. P.: Improved temperature response functions for models of Rubisco-limited photosynthesis, Plant, Cell & Environment, 24, 253–259, 2001.

35  Beven, K.: On doing better hydrological science, Hydrological Processes, 22, 3549–3553, 2008.

Bonan, G. B.: Forests and Climate Change: Forcings, Feedbacks, and the Climate Benefits of Forests, Science, 320, 1444–1449, https://doi.org/10.1126/science.1155121, http://science.sciencemag.org/content/320/5882/1444, 2008.

Bonan, G. B. and Doney, S. C.: Climate, ecosystems, and planetary futures: The challenge to predict life in Earth system models, Science, 359, https://doi.org/10.1126/science.aam8328, http://science.sciencemag.org/content/359/6375/eaam8328, 2018.

Bradford, M. A., Wieder, W. R., Bonan, G. B., Fierer, N., Raymond, P. A., and Crowther, T. W.: Managing uncertainty in soil carbon feedbacks to climate change, Nature Climate Change, 6, https://doi.org/10.1038/nclimate3071, http://dx.doi.org/10.1038/nclimate3071, 2016.

Brahney, J., Mahowald, N., Ward, D. S., Ballantyne, A. P., and Neff, J. C.: Is atmospheric phosphorus pollution altering global alpine Lake stoichiometry?, Global Biogeochemical Cycles, 29, 1369–1383, https://doi.org/10.1002/2015GB005137, https://agupubs.onlinelibrary.wiley.com/doi/abs/10.1002/2015GB005137, 2015.

Campioli, M., Vicca, S., Luyssaert, S., and Bilcke, J.: Biomass production efficiency controlled by management in temperate and boreal ecosystems, Nature Geoscience, 8, 843–846, 2015.

Carrara, A., Janssens, I. A., Yuste, J. C., and Ceulemans, R.: Seasonal changes in photosynthesis, respiration and NEE of a mixed temperate forest, Agricultural and Forest Meteorology, 126, 15 – 31, https://doi.org/https://doi.org/10.1016/j.agrformet.2004.05.002, http://www.sciencedirect.com/science/article/pii/S0168192304001145, 2004.

Chien, C.-T., Mackey, K. R. M., Dutkiewicz, S., Mahowald, N. M., Prospero, J. M., and Paytan, A.: Effects of African dust deposition on phytoplankton in the western tropical Atlantic Ocean off Barbados, Global Biogeochemical Cycles, 30, 716–734, https://doi.org/10.1002/2015GB005334, https://agupubs.onlinelibrary.wiley.com/doi/abs/10.1002/2015GB005334, 2016.

Chiesi, M., Maselli, F., Bindi, M., Fibbi, L., Cherubini, P., Arlotta, E., Tirone, G., Matteucci, G., and Seufert, G.: Modelling carbon budget of Mediterranean forests using ground and remote sensing measurements, Agricultural and Forest Meteorology, 135, 22 – 34, https://doi.org/https://doi.org/10.1016/j.agrformet.2005.09.011, http://www.sciencedirect.com/science/article/pii/S0168192305002108, 2005.

Clark, D. B., Mercado, L. M., Sitch, S. A., Jones, C. D., Gedney, N., Best, M. J., Pryor, M., Rooney, G. G., Essery, R. L. H., Blyth, E., Boucher, O., Harding, R. J., Huntingford, C., and Cox, P. M.: The Joint UK Land Environment Simulator (JULES), model description – Part 2: Carbon fluxes and vegetation dynamics, Geoscientific Model Development, 4, 701–722, 2011.

Cleugh, H. A., Leuning, R., Mu, Q., and Running, S. W.: Regional evaporation estimates from flux tower and MODIS satellite data, Remote Sensing of Environment, 106, 285 – 304, https://doi.org/https://doi.org/10.1016/j.rse.2006.07.007, http://www.sciencedirect.com/science/article/pii/S0034425706002677, 2007.

Cook, B. D., Davis, K. J., Wang, W., Desai, A., Berger, B. W., Teclaw, R. M., Martin, J. G., Bolstad, P. V., Bakwin, P. S., Yi, C., and Heilman, W.: Carbon exchange and venting anomalies in an upland deciduous forest in northern Wisconsin, USA, Agricultural and Forest Meteorology, 126, 271 – 295, https://doi.org/https://doi.org/10.1016/j.agrformet.2004.06.008, http://www.sciencedirect.com/science/article/pii/S0168192304001601, 2004.

Cornwell, W., Wright, I., Turner, J., Maire, V., Barbour, M., Cernusak, L., Dawson, T., Ellsworth, D., Farquhar, G., Griffiths, H., Keitel, C., Knohl, A., Reich, P., Williams, D., Bhaskar, R., Cornelissen, J., Richards, A., Schmidt, S., Valladares, F., C, K., Schulze, E.-D., Buchmann, N., and Santiago, L.: Leaf $\Delta^{13}$C database, https://github.com/wcornwell/leaf13C/tree/v0.1.0, 2018a.

Cornwell, W. K., Wright, I. J., Turner, J., Maire, V., Barbour, M. M., Cernusak, L. A., Dawson, T., Ellsworth, D., Farquhar, G. D., Griffiths, H., Keitel, C., Knohl, A., Reich, P. B., Williams, D. G., Bhaskar, R., Cornelissen, J. H. C., Richards, A., Schmidt, S., Valladares, F., Körner, C., Schulze, E.-D., Buchmann, N., and Santiago, L. S.: Climate and soils together regulate photosynthetic carbon isotope discrimination within C3 plants worldwide, Global Ecology and Biogeography, 27, 1056–1067, 2018b.

De Kauwe, M. G., Medlyn, B. E., Zaehle, S., Walker, A. P., Dietze, M. C., Hickler, T., Jain, A. K., Luo, Y., Parton, W. J., Prentice, I. C., Smith, B., Thornton, P. E., Wang, S., Wang, Y.-P., Wårlind, D., Weng, E., Crous, Kristine, Y., Ellsworth, D. S., Hanson, P. J., Seok, K. H., Warren, J. M., Oren, R., and Norby, R. J.: Forest water use and water use efficiency at elevated CO2: a model-data intercomparison at two contrasting temperate forest FACE sites, Global Change Biology, 19, 1759–1779, https://doi.org/10.1111/gcb.12164, https://onlinelibrary.
5      wiley.com/doi/abs/10.1111/gcb.12164, 2013.

De Kauwe, M. G., Medlyn, B. E., Zaehle, S., Walker, A. P., Dietze, M. C., Wang, Y.-P., Luo, Y., Jain, A. K., El-Masri, B., Hickler, T., Wårlind, D., Weng, E., Parton, W. J., Thornton, P. E., Wang, S., Prentice, I. C., Asao, S., Smith, B., McCarthy, H. R., Iversen, C. M., Hanson, P. J., Warren, J. M., Oren, R., and Norby, R. J.: Where does the carbon go? A model–data intercomparison of vegetation carbon allocation and turnover processes at two temperate forest free-air CO2 enrichment sites, New Phytologist, 203, 883–899,
10     https://doi.org/10.1111/nph.12847, https://nph.onlinelibrary.wiley.com/doi/abs/10.1111/nph.12847, 2014.

Desai, A. R., Bolstad, P. V., Cook, B. D., Davis, K. J., and Carey, E. V.: Comparing net ecosystem exchange of carbon dioxide between an old-growth and mature forest in the upper Midwest, USA, Agricultural and Forest Meteorology, 128, 33 – 55, https://doi.org/https://doi.org/10.1016/j.agrformet.2004.09.005, http://www.sciencedirect.com/science/article/pii/S0168192304002369, 2005.

15    Dickinson, R. E., Oleson, K. W., Bonan, G., Hoffman, F., Thornton, P., Vertenstein, M., Yang, Z.-L., and Zeng, X.: The Community Land Model and Its Climate Statistics as a Component of the Community Climate System Model, Journal of Climate, 19, 2302–2324, https://doi.org/10.1175/JCLI3742.1, https://doi.org/10.1175/JCLI3742.1, 2006.

Dolman, A., Moors, E., and Elbers, J.: The carbon uptake of a mid latitude pine forest growing on sandy soil, Agricultural and Forest Meteorology, 111, 157 – 170, https://doi.org/https://doi.org/10.1016/S0168-1923(02)00024-2, http://www.sciencedirect.com/science/article/
20     pii/S0168192302000242, 2002.

Dunn, A. L., Barford, C. C., Wofsy, S. C., Goulden, M. L., and Daube, B. C.: A long-term record of carbon exchange in a boreal black spruce forest: means, responses to interannual variability, and decadal trends, Global Change Biology, 13, 577–590, https://doi.org/10.1111/j.1365-2486.2006.01221.x, https://onlinelibrary.wiley.com/doi/abs/10.1111/j.1365-2486.2006.01221.x, 2007.

Fatichi, S., Leuzinger, S., and Körner, C.: Moving beyond photosynthesis: from carbon source to sink-driven vegetation modeling, New
25     Phytologist, 201, 1086–1095, 2013.

Fisher, R., McDowell, N., Purves, D., Moorcroft, P., Sitch, S. A., Cox, P. M., Huntingford, C., Meir, P., and Ian Woodward, F.: Assessing uncertainties in a second-generation dynamic vegetation model caused by ecological scale limitations, New Phytologist, 187, 666–681, 2010.

Friedlingstein, P., Meinshausen, M., Arora, V. K., Jones, C. D., Anav, A., Liddicoat, S. K., and Knutti, R.: Uncertainties in CMIP5 Climate
30     Projections due to Carbon Cycle Feedbacks, Journal of Climate, 27, 511–526, https://doi.org/10.1175/JCLI-D-12-00579.1, https://doi.org/
10.1175/JCLI-D-12-00579.1, 2014.

Friend, A. D.: Terrestrial plant production and climate change, Journal of Experimental Botany, 61, 1293–1309, 2010.

Friend, A. D., Geider, R. J., Behrenfeld, M. J., and Still, C. J.: Photosynthesis in Global-Scale Models, in: Photosynthesis in silico: Understanding complexity from molecules to ecosystems, edited by Laisk, A., Nedbal, L., and Govindjee, pp. 465–497, Springer, 2009.

35    Gerber, S., Hedin, L. O., Oppenheimer, M., Pacala, S. W., and Shevliakova, E.: Nitrogen cycling and feedbacks in a global dynamic land model, Global Biogeochemical Cycles, 24, GB1001 doi:10.1029–2008GB003 336, 2010.

Goldstein, A., Hultman, N., Fracheboud, J., Bauer, M., Panek, J., Xu, M., Qi, Y., Guenther, A., and Baugh, W.: Effects of climate variability on the carbon dioxide, water, and sensible heat fluxes above a ponderosa pine plantation in the Sierra Nevada (CA), Agricultural and For-

est Meteorology, 101, 113 – 129, https://doi.org/https://doi.org/10.1016/S0168-1923(99)00168-9, http://www.sciencedirect.com/science/article/pii/S0168192399001689, 2000.

Goll, D. S., Vuichard, N., Maignan, F., Jornet-Puig, A., Sardans, J., Violette, A., Peng, S., Sun, Y., Kvakic, M., Guimberteau, M., Guenet, B.,
Zaehle, S., Penuelas, J., Janssens, I., and Ciais, P.: A representation of the phosphorus cycle for ORCHIDEE (revision 4520), Geoscien-
5  tific Model Development, 10, 3745–3770, https://doi.org/10.5194/gmd-10-3745-2017, https://www.geosci-model-dev.net/10/3745/2017/,
2017.

Granier, A., Ceschia, E., Damesin, C., Dufrêne, E., Epron, D., Gross, P., Lebaube, S., Le Dantec, V., Le Goff, N., Lemoine, D., Lucot,
E., Ottorini, J. M., Pontailler, J. Y., and Saugier, B.: The carbon balance of a young Beech forest, Functional Ecology, 14, 312–325,
https://doi.org/10.1046/j.1365-2435.2000.00434.x, https://besjournals.onlinelibrary.wiley.com/doi/abs/10.1046/j.1365-2435.2000.00434.
10 x, 2000.

Graven, H., Allison, C. E., Etheridge, D. M., Hammer, S., Keeling, R. F., Levin, I., Meijer, H. A. J., Rubino, M., Tans, P. P., Trudinger, C. M.,
Vaughn, B. H., and White, J. W. C.: Compiled records of carbon isotopes in atmospheric $CO_2$ for historical simulations in CMIP6, Geo-
scientific Model Development, 10, 4405–4417, https://doi.org/10.5194/gmd-10-4405-2017, https://www.geosci-model-dev.net/10/4405/
2017/, 2017.

15 Gruber, N. and Galloway, J. N.: An Earth-system perspective of the global nitrogen cycle, Nature, 451, 293–296, 2008.

Grünwald, T. and Bernhofer, C.: A decade of carbon, water and energy flux measurements of an old spruce forest at the Anchor Sta-
tion Tharandt, Tellus B, 59, 387–396, https://doi.org/10.1111/j.1600-0889.2007.00259.x, https://onlinelibrary.wiley.com/doi/abs/10.1111/
j.1600-0889.2007.00259.x, 2007.

Grünzweig, J. M., Lin, T., Rotenberg, E., Schwartz, A., and Yakir, D.: Carbon sequestration in arid-land forest, Global Change Biology, 9,
20  791–799, https://doi.org/10.1046/j.1365-2486.2003.00612.x, https://onlinelibrary.wiley.com/doi/abs/10.1046/j.1365-2486.2003.00612.x,
2003.

Gu, L., Meyers, T., Pallardy, S. G., Hanson, P. J., Yang, B., Heuer, M., Hosman, K. P., Riggs, J. S., Sluss, D., and Wullschleger, S. D.:
Direct and indirect effects of atmospheric conditions and soil moisture on surface energy partitioning revealed by a prolonged drought
at a temperate forest site, Journal of Geophysical Research: Atmospheres, 111, https://doi.org/10.1029/2006JD007161, https://agupubs.
25  onlinelibrary.wiley.com/doi/abs/10.1029/2006JD007161, 2006.

Hararuk, O., Smith, M. J., and Luo, Y.: Microbial models with data-driven parameters predict stronger soil carbon responses to climate
change, Global Change Biology, 21, 2439–2453, https://doi.org/10.1111/gcb.12827, https://onlinelibrary.wiley.com/doi/abs/10.1111/gcb.
12827, 2015.

Hartmann, H., Adams, H. D., Hammond, W. M., Hoch, G., Landhäusser, S. M., Wiley, E., and Zaehle, S.: Identifying differences in carbohy-
30  drate dynamics of seedlings and mature trees to improve carbon allocation in models for trees and forests, Environmental and Experimental
Botany, 152, 7–18, 2018.

Hengl, T., Mendes de Jesus, J., Heuvelink, G. B., Ruiperez Gonzalez, M., and Kilibarda, M.: ISoilGrids250m: global gridded soil information
based on Machine Learning, PLoS ONE, 12, e0169 748, https://doi.org/10.1371/journal.pone.0169748, 2017.

Hollinger, D. Y., Goltz, S. M., Davidson, E. A., Lee, J. T., Tu, K., and Valentine, H. T.: Seasonal patterns and environmental control of carbon
35  dioxide and water vapour exchange in an ecotonal boreal forest, Global Change Biology, 5, 891–902, https://doi.org/10.1046/j.1365-
2486.1999.00281.x, https://onlinelibrary.wiley.com/doi/abs/10.1046/j.1365-2486.1999.00281.x, 1999.

Hou, E., Chen, C., Luo, Y., Zhou, G., Kuang, Y., Zhang, Y., Heenan, M., Lu, X., and Wen, D.: Effects of climate on soil phosphorus cycle and availability in natural terrestrial ecosystems, Global Change Biology, 24, 3344–3356, https://doi.org/10.1111/gcb.14093, https://onlinelibrary.wiley.com/doi/abs/10.1111/gcb.14093, 2018.

Hungate, B. A., Dukes, J. S., Shaw, M. R., Luo, Y., and Field, C. B.: Nitrogen and Climate Change, Science, 302, 1512–1513,
5  https://doi.org/10.1126/science.1091390, http://science.sciencemag.org/content/302/5650/1512, 2003.

Ilvesniemi, H., Levula, J., Ojansuu, R., Kolari, P., Kulmala, L., Pumpanen, J. Launiainen, S., Vesala, T., and Nikinmaa, E.: Long-term measurements of the carbon balance of a boreal Scots pine dominated forest ecosystem, Boreal Enrironment Research, 14, 731–753, 2009.

Jiang, M., Caldararu, S., Zaehle, S., Ellsworth, D. S., and Medlyn, B. E.: Towards a more physiological representation of vegetation phos-
10  phorus processes in land surface models, The New Phytologist, https://doi.org/10.1111/nph.15688, http://dx.doi.org/10.1111/nph.15688, 2019.

June, T., Evans, J. R., and Farquhar, G. D.: A simple new equation for the reversible temperature dependence of photosynthetic electron transport: a study on soybean leaf, Functional Plant Biology, 31, 275, 2004.

Kattge, J., Díaz, S., Lavorel, S., Prentice, I. C., Leadley, P., Bönisch, G., Garnier, E., Westoby, M., Reich, P. B., Wright, I. J., Cornelissen,
15  J. H. C., Violle, C., Harrison, S. P., Van Bodegom, P. M., Reichstein, M., Enquist, B. J., Soudzilovskaia, N. A., Ackerly, D. D., Anand, M., Atkin, O., Bahn, M., Baker, T. R., Baldocchi, D., Bekker, R., Blanco, C. C., Blonder, B., Bond, W. J., Bradstock, R., Bunker, D. E., Casanoves, F., Caverner-Bares, J., Chambers, J. Q., Chapin III, F. S., Chave, J., Coomes, D., Cornwell, W. K., Craine, J. M., Dobrin, B. H., Duarte, L., Durka, W., Elser, J., Esser, G., Estiarte, M., Fagan, W. F., Fand, J., Fernández-Méndez, F., Fidelis, A., Finegan, B., Flores, O., Ford, H., Frank, D., Freschet, G. T., Fyllas, N. M., Gallagher, R. V., Green, W. A., Gutierrez, A. G., Thomas, H., Higgins, S. I., Hodgson,
20  J. G., Jalili, A., Jansen, S., Joly, C. A., Kerkhoff, A. J., Kirkup, D., Kitajima, K., Kleyer, M., Klotz, S., Knops, J. M. H., Kramer, K., Kühn, I., Kurokawa, H., Laughlin, D., Lee, T. D., Leishman, M., Lens, F., Lenz, T., Lewis, S. L., Lloyd, J., Llusià, J., Louault, F., Ma, S., Mahecha, M. D., Manning, P., Massad, T., Medlyn, B. E., Messier, J., Moles, A. T., Müller, S. C., Nadrowski, K., Naeem, S., Niinemets, Ü., Nöllert, S., Nüske, A., Ogaya, R., Oleksyn, J., Onipchenko, V. G., Onoda, Y., Ordoñez, J., Overbeck, G., Ozinga, W. A., Patino, S., Paula, S., Pausas, J. G., Peñuelas, J., Phillips, O. L., Pillar, V., Poorter, H., Poorter, L., Poschlod, P., Prinzing, A., Proulx, R., Rammig, A.,
25  Reinsch, S., Reu, B., Sack, L., Salgado-Negret, B., Sardans, J., Shiodera, S., Shipley, B., Siefert, A., Sosinski, E., Soussana, J. F., Swaine, E., Swenson, N., Thompson, K., Thornton, P., Waldram, M., Weiher, E., White, M., White, S., Wright, S. J., Yguel, B., Zaehle, S., Zanne, A. E., and Wirth, C.: TRY - a global database of plant traits, Global Change Biology, 17, 2905–2935, 2011.

Keenan, T., Sabate, S., and Gracia, C.: Soil water stress and coupled photosynthesis–conductance models: Bridging the gap between conflict-ing reports on the relative roles of stomatal, mesophyll conductance and biochemical limitations to photosynthesis, Agricultural and For-
30  est Meteorology, 150, 443 – 453, https://doi.org/https://doi.org/10.1016/j.agrformet.2010.01.008, http://www.sciencedirect.com/science/article/pii/S0168192310000110, 2010.

Knauer, J., Werner, C., and Zaehle, S.: Evaluating stomatal models and their atmospheric drought response in a land surface scheme: A multibiome analysis, Journal of Geophysical Research: Biogeosciences, 120, 1894–1911, 2015.

Knauer, J., Zaehle, S., Reichstein, M., Medlyn, B. E., Forkel, M., Hagemann, S., and Werner, C.: The response of ecosystem water-use
35  efficiency to rising atmospheric CO2 concentrations: sensitivity and large-scale biogeochemical implications, New Phytologist, 213, 1654–1666, https://doi.org/10.1111/nph.14288, https://nph.onlinelibrary.wiley.com/doi/abs/10.1111/nph.14288, 2016.

Knauer, J., Zaehle, S., De Kauwe, M., Bahar, N. H., Evans, J. R., Medlyn, B. E., Reichstein, M., and Werner, C.: Effects of mesophyll conductance on vegetation responses to elevated CO2 concentrations in a land surface model, Global Change Biology, in press.

Korhonen, J. F. J., Pihlatie, M., Pumpanen, J., Aaltonen, H., Hari, P., Levula, J., Kieloaho, A.-J., Nikinmaa, E., Vesala, T., and Ilvesniemi, H.: Nitrogen balance of a boreal Scots pine forest, Biogeosciences, 10, 1083–1095, https://doi.org/10.5194/bg-10-1083-2013, https://www.biogeosciences.net/10/1083/2013/, 2013.

Koven, C. D., Riley, W. J., Subin, Z. M., Tang, J. Y., Torn, M. S., Collins, W. D., Bonan, G. B., Lawrence, D. M., and Swenson, S. C.: The effect of vertically resolved soil biogeochemistry and alternate soil C and N models on C dynamics of CLM4, Biogeosciences, 10, 7109–7131, 2013.

Krinner, G., Viovy, N., de Noblet-Ducoudré, N., Ogée, J., Polcher, J., Friedlingstein, P., Ciais, P., Sitch, S. A., and Prentice, I. C.: A dynamic global vegetation model for studies of the coupled atmosphere-biosphere system, Global Biogeochemical Cycles, 19, GB1015, 2005.

Kull, O. and Kruijt, B.: Leaf photosynthetic light response: a mechanistic model for scaling photosynthesis to leaves and canopies, Functional Ecology, 12, 767–777, 1998.

Kutsch, W. L., Kolle, O., Rebmann, C., Knohl, A., Ziegler, W., and Schulze, E.-D.: Advection and resulting CO2 exchange uncertainty in a tall forest in central Germany, Ecological Applications, 18, 1391–1405, https://doi.org/10.1890/06-1301.1, https://esajournals.onlinelibrary.wiley.com/doi/abs/10.1890/06-1301.1, 2008.

Lagergren, F., Lindroth, A., Dellwik, E., Ibrom, A., Lankreijer, H., Launiainen, S., Mölder, M., Kolari, P., Pilegaard, K., and Vesala, T.: Biophysical controls on CO2 fluxes of three Northern forests based on long-term eddy covariance data, Tellus B, 60, 143–152, https://doi.org/10.1111/j.1600-0889.2006.00324.x, https://onlinelibrary.wiley.com/doi/abs/10.1111/j.1600-0889.2006.00324.x, 2008.

Lamarque, J.-F., Bond, T. C., Eyring, V., Granier, C., Heil, A., Klimont, Z., Lee, D., Liousse, C., Mieville, A., Owen, B., Schultz, M. G., Shindell, D., Smith, S. J., Stehfest, E., Van Aardenne, J., Cooper, O. R., Kainuma, M., Mahowald, N., McConnell, J. R., Naik, V., Riahi, K., and van Vuuren, D. P.: Historical (1850–2000) gridded anthropogenic and biomass burning emissions of reactive gases and aerosols: methodology and application, Atmospheric Chemistry and Physics, 10, 7017–7039, https://doi.org/10.5194/acp-10-7017-2010, https://www.atmos-chem-phys.net/10/7017/2010/, 2010.

Lamarque, J.-F., Kyle, G. P., Meinshausen, M., Riahi, K., Smith, S. J., van Vuuren, D. P., Conley, A. J., and Vitt, F.: Global and regional evolution of short-lived radiatively-active gases and aerosols in the Representative Concentration Pathways, Climatic Change, 109, 191, https://doi.org/10.1007/s10584-011-0155-0, https://doi.org/10.1007/s10584-011-0155-0, 2011.

Le Quéré, C., Andrew, R. M., Friedlingstein, P., Sitch, S., Pongratz, J., Manning, A. C., Korsbakken, J. I., Peters, G. P., Canadell, J. G., Jackson, R. B., Boden, T. A., Tans, P. P., Andrews, O. D., Arora, V. K., Bakker, D. C. E., Barbero, L., Becker, M., Betts, R. A., Bopp, L., Chevallier, F., Chini, L. P., Ciais, P., Cosca, C. E., Cross, J., Currie, K., Gasser, T., Harris, I., Hauck, J., Haverd, V., Houghton, R. A., Hunt, C. W., Hurtt, G., Ilyina, T., Jain, A. K., Kato, E., Kautz, M., Keeling, R. F., Klein Goldewijk, K., Körtzinger, A., Landschützer, P., Lefèvre, N., Lenton, A., Lienert, S., Lima, I., Lombardozzi, D., Metzl, N., Millero, F., Monteiro, P. M. S., Munro, D. R., Nabel, J. E. M. S., Nakaoka, S.-I., Nojiri, Y., Padin, X. A., Peregon, A., Pfeil, B., Pierrot, D., Poulter, B., Rehder, G., Reimer, J., Rödenbeck, C., Schwinger, J., Séférian, R., Skjelvan, I., Stocker, B. D., Tian, H., Tilbrook, B., Tubiello, F. N., van der Laan-Luijkx, I. T., van der Werf, G. R., van Heuven, S., Viovy, N., Vuichard, N., Walker, A. P., Watson, A. J., Wiltshire, A. J., Zaehle, S., and Zhu, D.: Global Carbon Budget 2017, Earth System Science Data, 10, 405–448, https://doi.org/10.5194/essd-10-405-2018, https://www.earth-syst-sci-data.net/10/405/2018/, 2018.

LeBauer, D. S. and Treseder, K. K.: Nitrogen limitation of net primary productivity in terrestrial ecosystems is globally distributed, Ecology, 89, 371–379, 2008.

Lin, Y.-S., Medlyn, B. E., Duursma, R. A., Prentice, I. C., Wang, H., Baig, S., Eamus, D., de Dios, V. R., Mitchell, P., Ellsworth, D. S., de Beeck, M. O., Wallin, G., Uddling, J., Tarvainen, L., Linderson, M.-L., Cernusak, L. A., Nippert, J. B., Ocheltree, T. W., Tissue, D. T.,

Martin-StPaul, N. K., Rogers, A., Warren, J. M., De Angelis, P., Hikosaka, K., Han, Q., Onoda, Y., Gimeno, T. E., Barton, C. V. M., Bennie, J., Bonal, D., Bosc, A., Low, M., Macinins-Ng, C., Rey, A., Rowland, L., Setterfield, S. A., Tausz-Posch, S., Zaragoza-Castells, J., Broadmeadow, M. S. J., Drake, J. E., Freeman, M., Ghannoum, O., Hutley, L. B., Kelly, J. W., Kikuzawa, K., Kolari, P., Koyama, K., Limousin, J. M., Meir, P., Lola da Costa, A. C., Mikkelsen, T. N., Salinas, N., Sun, W., and Wingate, L.: Optimal stomatal behaviour around the world, Nature Climate Change, 5, 459–464, 2015.

Lindroth, A., Klemedtsson, L., Grelle, A., Weslien, P., and Langvall, O.: Measurement of net ecosystem exchange, productivity and respiration in three spruce forests in Sweden shows unexpectedly large soil carbon losses, Biogeochemistry, 89, 43–60, https://doi.org/10.1007/s10533-007-9137-8, https://doi.org/10.1007/s10533-007-9137-8, 2008.

Lloyd, J. and Taylor, J. A.: On the temperature dependence of soil respiration, Functional ecology, pp. 315–323, https://www.jstor.org/stable/2389824, 1994.

Ma, S., Baldocchi, D. D., Xu, L., and Hehn, T.: Inter-annual variability in carbon dioxide exchange of an oak/grass savanna and open grassland in California, Agricultural and Forest Meteorology, 147, 157 – 171, https://doi.org/https://doi.org/10.1016/j.agrformet.2007.07.008, http://www.sciencedirect.com/science/article/pii/S016819230700189X, 2007.

Mauritsen, T., Bader, J., Becker, T., Behrens, J., Bittner, M., Brokopf, R., Brovkin, V., Claussen, M., Crueger, T., Esch, M., Fast, I., Fiedler, S., Fläschner, D., Gayler, V., Giorgetta, M., Goll, D. S., Haak, H., Hagemann, S., Hedemann, C., Hohenegger, C., Ilyina, T., Jahns, T., Jimenez de la Cuesta Otero, D., Jungclaus, J., Kleinen, T., Kloster, S., Kracher, D., Kinne, S., Kleberg, D., Lasslop, G., Kornblueh, L., Marotzke, J., Matei, D., Meraner, K., Mikolajewicz, U., Modali, K., Möbis, B., Müller, W. A., Nabel, J. E. M. S., Nam, C. C. W., Notz, D., Nyawira, S.-S., Paulsen, H., Peters, K., Pincus, R., Pohlmann, H., Pongratz, J., Popp, M., Raddatz, T., Rast, S., Redler, R., Reick, C. H., Rohrschneider, T., Schemann, V., Schmidt, H., Schnur, R., Schulzweida, U., Six, K. D., Stein, L., Stemmler, I., Stevens, B., von Storch, J.-S., Tian, F., Voigt, A., de Vrese, P., Wieners, K.-H., Wilkenskjeld, S., Winkler, A., and Roeckner, E.: Developments in the MPI-M Earth System Model version 1.2 (MPI-ESM 1.2) and its response to increasing $CO_2$, Journal of Advances in Modeling Earth Systems, pp. 1–110, 2019.

Medlyn, B. E., Zaehle, S., De Kauwe, M. G., Walker, A. P., Dietze, M. C., Hanson, P. J., Hickler, T., Jain, A. K., Luo, Y., Parton, W., Prentice, I. C., Thornton, P. E., Wang, S., Wang, Y.-P., Weng, E., Iversen, C. M., McCarthy, H. R., Warren, J. M., Oren, R., and Norby, R. J.: Using ecosystem experiments to improve vegetation models, Nature Climate Change, 5, 528–534, 2015.

Medlyn, B. E., De Kauwe, M. G., Zaehle, S., Walker, A. P., Duursma, R. A., Luus, K., Mishurov, M., Pak, B., Smith, B., Wang, Y.-P., Yang, X., Crous, K. Y., Drake, J. E., Gimeno, T. E., Macdonald, C. A., Norby, R. J., Power, S. A., Tjoelker, M. G., and Ellsworth, D. S.: Using models to guide field experiments: a priori predictions for the $CO_2$ response of a nutrient- and water-limited native Eucalypt woodland, Global Change Biology, 22, 2834–2851, 2016.

Medlyn, B. E., De Kauwe, M. G., Lin, Y.-S., Knauer, J., Duursma, R. A., Williams, C. A., Arneth, A., Clement, R., Isaac, P., Limousin, J. M., Linderson, M.-L., Meir, P., Martin-StPaul, N., and Wingate, L.: How do leaf and ecosystem measures of water-use efficiency compare?, New Phytologist, 216, 758–770, 2017.

Mercado, L. M., Medlyn, B. E., Huntingford, C., Oliver, R. J., Clark, D. B., Sitch, S. A., Zelazowski, P., Kattge, J., Harper, A. B., and Cox, P. M.: Large sensitivity in land carbon storage due to geographical and temporal variation in the thermal response of photosynthetic capacity., The New phytologist, 218, 1462–1477, 2018.

Mkhabela, M., Amiro, B., Barr, A., Black, T., Hawthorne, I., Kidston, J., McCaughey, J., Orchansky, A., Nesic, Z., Sass, A., Shashkov, A., and Zha, T.: Comparison of carbon dynamics and water use efficiency following fire and harvesting in Canadian boreal forests, Agricultural

and Forest Meteorology, 149, 783 – 794, https://doi.org/https://doi.org/10.1016/j.agrformet.2008.10.025, http://www.sciencedirect.com/science/article/pii/S0168192308003080, 2009.

NOA: FLUXNET Data Download, http://www.fluxdata.org/DataDownload/default.aspx, last access: 17 February 2015, 2007.

Papale, D., Reichstein, M., Aubinet, M., Canfora, E., Bernhofer, C., Kutsch, W., Longdoz, B., Rambal, S., Valentini, R., Vesala, T., and Yakir,
5    D.: Towards a standardized processing of Net Ecosystem Exchange measured with eddy covariance technique: algorithms and uncertainty
     estimation, Biogeosciences, 3, 571–583, https://doi.org/10.5194/bg-3-571-2006, https://www.biogeosciences.net/3/571/2006/, 2006.

Parton, W. J., Scurlock, J. M. O., Ojima, D. S., Gilmanov, T. G., Scholes, R. J., Schimmel, D. S., Kirchner, T., Menaut, J. C., Seastedt,
     T., Moya, E. G., Kamnalrut, A., and Kinyamario, J. I.: Observations and modelling of biomass and soil organic matter dynamics for the
     grassland biome worldwide, Global Biogeochemical Cycles, 7, 785–809, 1993.

10   Peng, J., Dan, L., and Huang, M.: Sensitivity of Global and Regional Terrestrial Carbon Storage to the Direct CO2 Effect and Climate
     Change Based on the CMIP5 Model Intercomparison, PLOS ONE, 9, 1–17, https://doi.org/10.1371/journal.pone.0095282, https://doi.org/
     10.1371/journal.pone.0095282, 2014.

Peñuelas, J., Poulter, B., Sardans, J., Ciais, P., van der Velde, M., Bopp, L., Boucher, O., Godderis, Y., Hinsinger, P., Llusia, Joan Nardin, E.,
     Vicca, S., Obersteiner, M., and Janssens, I. A.: Human-induced nitrogen–phosphorus imbalances alter natural and managed ecosystems
15   across the globe, Nature Communications, 4, https://doi.org/10.1038/ncomms3934, http://dx.doi.org/10.1038/ncomms3934, 2013.

Prentice, I. C., Liang, X., Medlyn, B. E., and Wang, Y. P.: Reliable, robust and realistic: the three R's of next-generation land-surface
     modelling, Atmospheric Chemistry and Physics, 15, 5987–6005, 2015.

Raddatz, T. J., Reick, C. H., Knorr, W., Kattge, J., Roeckner, E., Schnur, R., Schnitzler, K.-G., Wetzel, P., and Jungclaus, J.: Will the
     tropical land biosphere dominate the climate–carbon cycle feedback during the twenty-first century?, Climate Dynamics, 29, 565–574,
20   https://doi.org/10.1007/s00382-007-0247-8, https://doi.org/10.1007/s00382-007-0247-8, 2007.

Rebmann, C., Anthoni, P., E., F., Göckede, M., Mangold, A., Subke, J.-A., Thomas, C., Wichura, B., Schulze, E.-D., Tenhunen, J. D., and
     Foken, T.: Carbon Budget of a Spruce Forest Ecosystem, in: Biogeochemistry of Forested Catchments in a Changing Environment, edited
     by Matzner, E., pp. 143–159, Springer, https://doi.org/https://doi.org/10.1007/978-3-662-06073-5_8, 2004.

Reed, S. C., Townsend, A. R., Taylor, P. G., and Cleveland, C. C.: Phosphorus Cycling in Tropical Forests Growing on Highly Weathered
25   Soils, in: Phosphorus in Action Biological Processes in Soil Phosphorus Cycling, edited by Bünemann, E., Oberson, A., and Frossard, E.,
     pp. 339–369, Springer Berlin Heidelberg, Berlin, Heidelberg, https://doi.org/10.1007/978-3-642-15271-9, 2011.

Reichstein, M., Falge, E., Baldocchi, D., Papale, D., Aubinet, M., Berbigier, P., Bernhofer, C., Buchmann, N., Gilmanov, T., Granier, A.,
     Grünwald, T., Havránková, K., Ilvesniemi, H., Janous, D., Knohl, A., Laurila, T., Lohila, A., Loustau, D., Matteucci, G., Meyers, T.,
     Miglietta, F., Ourcival, J.-M., Pumpanen, J., Rambal, S., Rotenberg, E., Sanz, M., Tenhunen, J., Seufert, G., Vaccari, F., Vesala, T., Yakir,
30   D., and Valentini, R.: On the separation of net ecosystem exchange into assimilation and ecosystem respiration: review and improved
     algorithm, Global Change Biology, 11, 1424–1439, https://doi.org/10.1111/j.1365-2486.2005.001002.x, https://onlinelibrary.wiley.com/
     doi/abs/10.1111/j.1365-2486.2005.001002.x, 2005.

Roupsard, O., Bonnefond, J.-M., Irvine, M., Berbigier, P., Nouvellon, Y., Dauzat, J., Taga, S., Hamel, O., Jourdan, C., Saint-
     André, L., Mialet-Serra, I., Labouisse, J.-P., Epron, D., Joffre, R., Braconnier, S., Rouzière, A., Navarro, M., and Bouillet,
35   J.-P.: Partitioning energy and evapo-transpiration above and below a tropical palm canopy, Agricultural and Forest Meteorol-
     ogy, 139, 252 – 268, https://doi.org/https://doi.org/10.1016/j.agrformet.2006.07.006, http://www.sciencedirect.com/science/article/pii/
     S0168192306001663, 2006.

Saltelli, A., Chan, K., and Scott, E. M.: Sensitivity Analysis, John Wiley & Sons, ltd., Chichester, New York, 2000.

Sanz, M., Carrara, A., Gimeno, C., Bucher, A., and Lopez, R.: Effects of a dry and warm summer conditions on $CO_2$ and energy fluxes from three Mediterranean ecosystems, Geophysical Research Abstracts, 6, 3239–3239, 2004.

Saxton, K. E. and Rawls, W. J.: Soil Water Characteristic Estimates by Texture and Organic Matter for Hydrologic Solutions, Soil Science Society of America Journal, 70, 1569–10, 2006.

5   Scherer-Lorenzen, M., Schulze, E.-D., Don, A., Schumacher, J., and Weller, E.: Exploring the functional significance of forest diversity: A new long-term experiment with temperate tree species (BIOTREE), Perspectives in Plant Ecology, Evolution and Systematics, 9, 53 – 70, https://doi.org/https://doi.org/10.1016/j.ppees.2007.08.002, http://www.sciencedirect.com/science/article/pii/S1433831907000339, 2007.

Schmid, H. P., Grimmond, C. B., Cropley, F., Offerle, B., and Su, H.-B.: Measurements of CO2 and energy fluxes over a mixed hardwood forest in the mid-western United States, Agricultural and Forest Meteorology, 103, 357 – 374, https://doi.org/https://doi.org/10.1016/S0168-
10   1923(00)00140-4, http://www.sciencedirect.com/science/article/pii/S0168192300001404, 2000.

Scott, R. L., Jenerette, G. D., Potts, D. L., and Huxman, T. E.: Effects of seasonal drought on net carbon dioxide exchange from a woody-plant-encroached semiarid grassland, Journal of Geophysical Research: Biogeosciences, 114, https://doi.org/10.1029/2008JG000900, https://agupubs.onlinelibrary.wiley.com/doi/abs/10.1029/2008JG000900, 2009.

Shinozaki, K., Yoda, K., Hozumi, K., and Kira, T.: A quantitative analysis of the plant form - the pipe model theory, Japanes Journal of
15   Ecology, 14, 98–104, 1964.

Sitch, S., Friedlingstein, P., Gruber, N., Jones, S. D., Murray-Tortarolo, G., Ahlström, A., Doney, S. C., Graven, H., Heinze, C., Huntingford, C., Levis, S., Levy, P. E., Lomas, M., Poulter, B., Viovy, N., Zaehle, S., Zeng, N., Arneth, A., Bonan, G., Bopp, L., Canadell, J. G., Chevallier, F., Ciais, P., Ellis, R., Gloor, M., Peylin, P., Piao, S. L., Le Quere, C., Smith, B., Zhu, Z., and Myneni, R.: Recent trends and drivers of regional sources and sinks of carbon dioxide, Biogeosciences, 12, 653–679, https://doi.org/10.5194/bg-12-653-2015, https:
20   //www.biogeosciences.net/12/653/2015/, 2015.

Sitch, S. A., Smith, B., Prentice, I. C., Arneth, A., Bondeau, A., Cramer, W., Kaplan, J. O., Levis, S., Lucht, W., Sykes, M. T., and Venevsky, S.: Evaluation of ecosystem dynamics, plant geography and terrestrial carbon cycling in the LPJ Dynamic Global Vegetation Model, Global Change Biology, 9, 161–185, 2003.

Suni, T., Rinne, J., Reissell, A., Altimir, N., Keronen, P., Rannik, Ü., Dal Maso, M., Kulmala, M., and Vesala, T.: Long-term measurements
25   of surface fluxes above a Scots pine forest in Hyytiälä, southern Finland, 1996-2001, Boreal Enrironment Research, 8, 287–301, 2003.

Swann, A. L. S., Hoffman, F. M., Koven, C. D., and Randerson, J. T.: Plant responses to increasing CO2 reduce estimates of climate impacts on drought severity, Proceedings of the National Academy of Sciences, 113, 10 019–10 024, https://doi.org/10.1073/pnas.1604581113, http://www.pnas.org/content/113/36/10019, 2016.

Tedeschi, V., Rey, A., Manca, G., Valentini, R., Jarvis, P. G., and Borghetti, M.: Soil respiration in a Mediterranean oak forest at different
30   developmental stages after coppicing, Global Change Biology, 12, 110–121, https://doi.org/10.1111/j.1365-2486.2005.01081.x, https://onlinelibrary.wiley.com/doi/abs/10.1111/j.1365-2486.2005.01081.x, 2006.

Thornton, P., Lamarque, J.-F., Rosenbloom, N. A., and Mahowald, N. M.: Influence of carbon-nitrogen cycle coupling on land model response to CO2 fertilization and climate variability, Global Biogeochemical Cycles, 21, https://doi.org/10.1029/2006GB002868, https://agupubs.onlinelibrary.wiley.com/doi/abs/10.1029/2006GB002868, 2007.

35   Thum, T., Zaehle, S., Köhler, P., Aalto, T., Aurela, M., Guanter, L., Kolari, P., Laurila, T., Lohila, A., Magnani, F., Van Der Tol, C., and Markkanen, T.: Modelling sun-induced fluorescence and photosynthesis with a land surface model at local and regional scales in northern Europe, Biogeosciences, 14, 1969–1987, https://doi.org/10.5194/bg-14-1969-2017, https://www.biogeosciences.net/14/1969/2017/, 2017.

Tirone, G., Dore, S., Matteucci, G., Greco, S., and Valentini, R.: Evergreen Mediterranean Forests. Carbon and Water Fluxes, Balances, Ecological and Ecophysiological Determinants, in: Fluxes of Carbon, Water and Energy of European Forests, edited by Valentini, R., pp. 125–149, Springer Berlin Heidelberg, Berlin, Heidelberg, https://doi.org/10.1007/978-3-662-05171-9_7, https://doi.org/10.1007/978-3-662-05171-9_7, 2003.

5  Urbanski, S., Barford, C., Wofsy, S., Kucharik, C., Pyle, E., Budney, J., McKain, K., Fitzjarrald, D., Czikowsky, M., and Munger, J. W.: Factors controlling CO2 exchange on timescales from hourly to decadal at Harvard Forest, Journal of Geophysical Research: Biogeosciences, 112, https://doi.org/10.1029/2006JG000293, https://agupubs.onlinelibrary.wiley.com/doi/abs/10.1029/2006JG000293, 2007.

Vargas, R., Sonnentag, O., Abramowitz, G., Carrara, A., Chen, J. M., Ciais, P., Correia, A., Keenan, T. F., Kobayashi, H., Ourcival, J.-M., Papale, D., Pearson, D., Pereira, J. S., Piao, S., Rambal, S., and Baldocchi, D. D.: Drought Influences the Accuracy of Simulated Ecosystem

10  Fluxes: A Model-Data Meta-analysis for Mediterranean Oak Woodlands, Ecosystems, 16, 749–764, https://doi.org/10.1007/s10021-013-9648-1, https://doi.org/10.1007/s10021-013-9648-1, 2013.

Vicca, S., Luyssaert, S., Peñuelas, J., Campioli, M., Chapin III, F. S., Ciais, P., Heinemeyer, A., Hogberg, P., Kutsch, W. L., Law, B. E., Malhi, Y., Papale, D., Piao, S. L., Reichstein, M., Schulze, E. D., and Janssens, I. A.: Fertile forests produce biomass more efficiently, Ecology Letters, 15, 520–526, 2012.

15  Viovy, N.: CRU-NCEP dataset, v7, https://vesg.ipsl.upmc.fr/thredds/catalog/store/p529viov/cruncep/V7_1901_2015/catalog.html, 2016.

Vitousek, P. M. and Howarth, R. W.: Nitrogen limitation on land and in the sea - how it can occur, Biogeochemistry, 13, 87–115, 1991.

Vitousek, P. M., Porder, S., Houlton, B. Z., and Chadwick, O. A.: Terrestrial phosphorus limitation: mechanisms, implications, and nitrogen–phosphorus interactions, Ecological Applications, 20, 5–15, https://doi.org/10.1890/08-0127.1, 2010.

Walker, T. W. and Syers, J. K.: The fate of phosphorus during pedogenesis, Geoderma, 15, 1–19, https://doi.org/10.1016/0016-7061(76)90066-5, http://linkinghub.elsevier.com/retrieve/pii/0016706176900665, 1976.

Wang, Y. P., Law, R. M., and Pak, B.: A global model of carbon, nitrogen and phosphorus cycles for the terrestrial biosphere, Biogeosciences, 7, 2261–2282, 2010.

Warlind, D., Smith, B., Hickler, T., and Arneth, A.: Nitrogen feedbacks increase future terrestrial ecosystem carbon uptake in an individual-based dynamic vegetation model, Biogeosciences, 11, 6131–6146, 2014.

25  White, R. E.: Principles and Practice of Soil Science The soil as a Natural Resource, vol. 32, Blackwell Publishing, Malden, 4th edn., https://doi.org/10.1177/0340035206070163, 2006.

Wohlfahrt, G., Anderson-Dunn, M., Bahn, M., Balzarolo, M., Berninger, F., Campbell, C., Carrara, A., Cescatti, A., Christensen, T., Dore, S., Eugster, W., Friborg, T., Furger, M., Gianelle, D., Gimeno, C., Hargreaves, K., Hari, P., Haslwanter, A., Johansson, T., Marcolla, B., Milford, C., Nagy, Z., Nemitz, E., Rogiers, N., Sanz, M. J., Siegwolf, R. T., Susiluoto, S., Sutton, M., Tuba, Z., Ugolini, F., Valentini, R., Zorer,

30  R., and Cernusca, A.: Biotic, Abiotic, and Management Controls on the Net Ecosystem CO2 Exchange of European Mountain Grassland Ecosystems, Ecosystems, 11, 1338–1351, https://doi.org/10.1007/s10021-008-9196-2, https://doi.org/10.1007/s10021-008-9196-2, 2008a.

Wohlfahrt, G., Hammerle, A., Haslwanter, A., Bahn, M., Tappeiner, U., and Cernusca, A.: Seasonal and inter-annual variability of the net ecosystem CO2 exchange of a temperate mountain grassland: Effects of weather and management, Journal of Geophysical Research: At-

35  mospheres, 113, https://doi.org/10.1029/2007JD009286, https://agupubs.onlinelibrary.wiley.com/doi/abs/10.1029/2007JD009286, 2008b.

Yang, X., Post, W. M., Thornton, P. E., and Jain, A.: The distribution of soil phosphorus for global biogeochemical modeling, Biogeosciences, 10, 2525–2537, https://doi.org/10.5194/bg-10-2525-2013, 2013.

Yang, X., Thornton, P. E., Ricciuto, D. M., and Post, W. M.: The role of phosphorus dynamics in tropical forests – a modeling study using CLM-CNP, Biogeosciences, 11, 1667–1681, https://doi.org/10.5194/bg-11-1667-2014, https://www.biogeosciences.net/11/1667/2014/, 2014.

Zaehle, S. and Dalmonech, D.: Carbon–nitrogen interactions on land at global scales: current understanding in modelling climate biosphere feedbacks, Current Opinion in Environmental Sustainability, 3, 311–320, 2011.

Zaehle, S. and Friend, A. D.: Carbon and nitrogen cycle dynamics in the O-CN land surface model: 1. Model description, site-scale evaluation, and sensitivity to parameter estimates, Global Biogeochemical Cycles, 24, GB 1005, 2010.

Zaehle, S., Sitch, S. A., Smith, B., and Hatterman, F.: Effects of parameter uncertainties on the modeling of terrestrial biosphere dynamics, Global Biogeochemical Cycles, 19, doi:10.1029–2004GB002 395, https://doi.org/doi:10.1029/2004GB002395, 2005.

Zaehle, S., Friedlingstein, P., and Friend, A. D.: Terrestrial nitrogen feedbacks may accelerate future climate change, Geophysical Research Letters, 37, https://doi.org/10.1029/2009GL041345, https://agupubs.onlinelibrary.wiley.com/doi/abs/10.1029/2009GL041345, 2010.

Zaehle, S., Ciais, P., Friend, A. D., and Prieur, V.: Carbon benefits of anthropogenic reactive nitrogen offset by nitrous oxide emissions, Nature Geoscience, 4, 601–605, 2011.

Zaehle, S., Medlyn, B. E., De Kauwe, M. G., Walker, A. P., Dietze, M. C., Hickler, T., Luo, Y., Wang, Y.-P., El-Masri, B., Thornton, P., Jain, A., Wang, S., Warlind, D., Weng, E., Parton, W., Iversen, C. M., Gallet-Budynek, A., McCarthy, H., Finzi, A., Hanson, P. J., Prentice, I. C., Oren, R., and Norby, R. J.: Evaluation of 11 terrestrial carbon–nitrogen cycle models against observations from two temperate Free-Air CO2 Enrichment studies, New Phytologist, 202, 803–822, https://doi.org/10.1111/nph.12697, https://nph.onlinelibrary.wiley.com/doi/abs/10.1111/nph.12697, 2014.
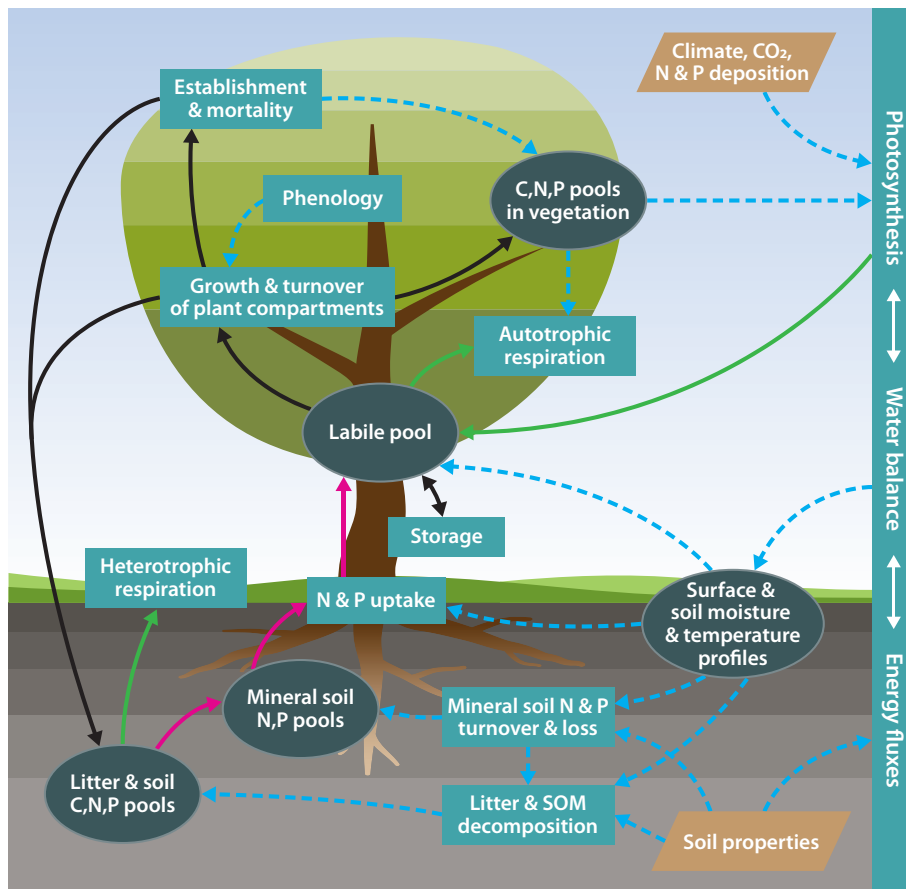
**Figure 1.** Schematic representation of the model structure. Elipses: biogeochemical pools and other state variables; rectangles: biogeochemical processes; tetraeders: model input; solid green lines: carbon fluxes; solid dark red lines: nitrogen and phosphorus fluxes; solid black lines: carbon, nitrogen and phosphorus fluxes; dotted blue lines: effects.
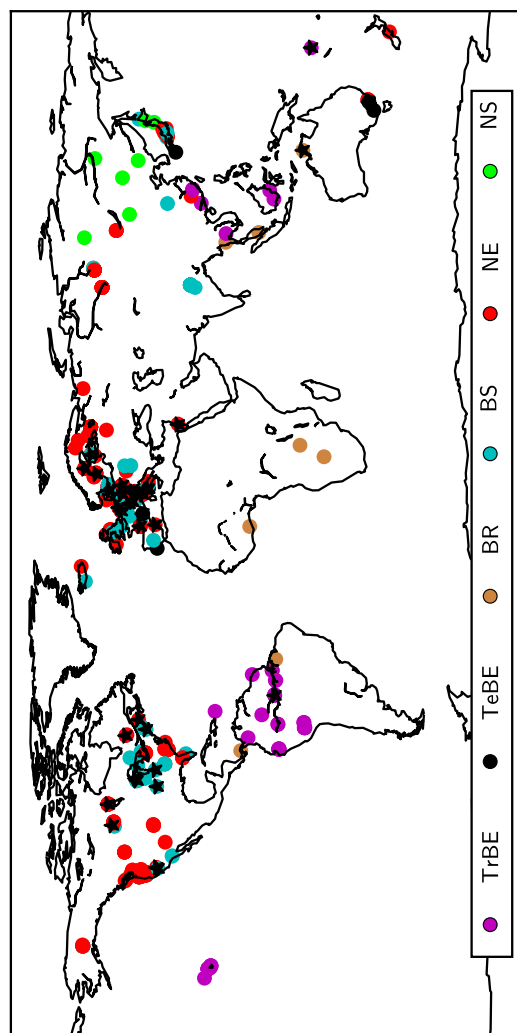
**Figure 2.** Locations of the sites used for model evaluation. Black stars: FLUXNET sites; circles: GFDB sites with circles having colors corresponding to different PFTs (see Table 1).
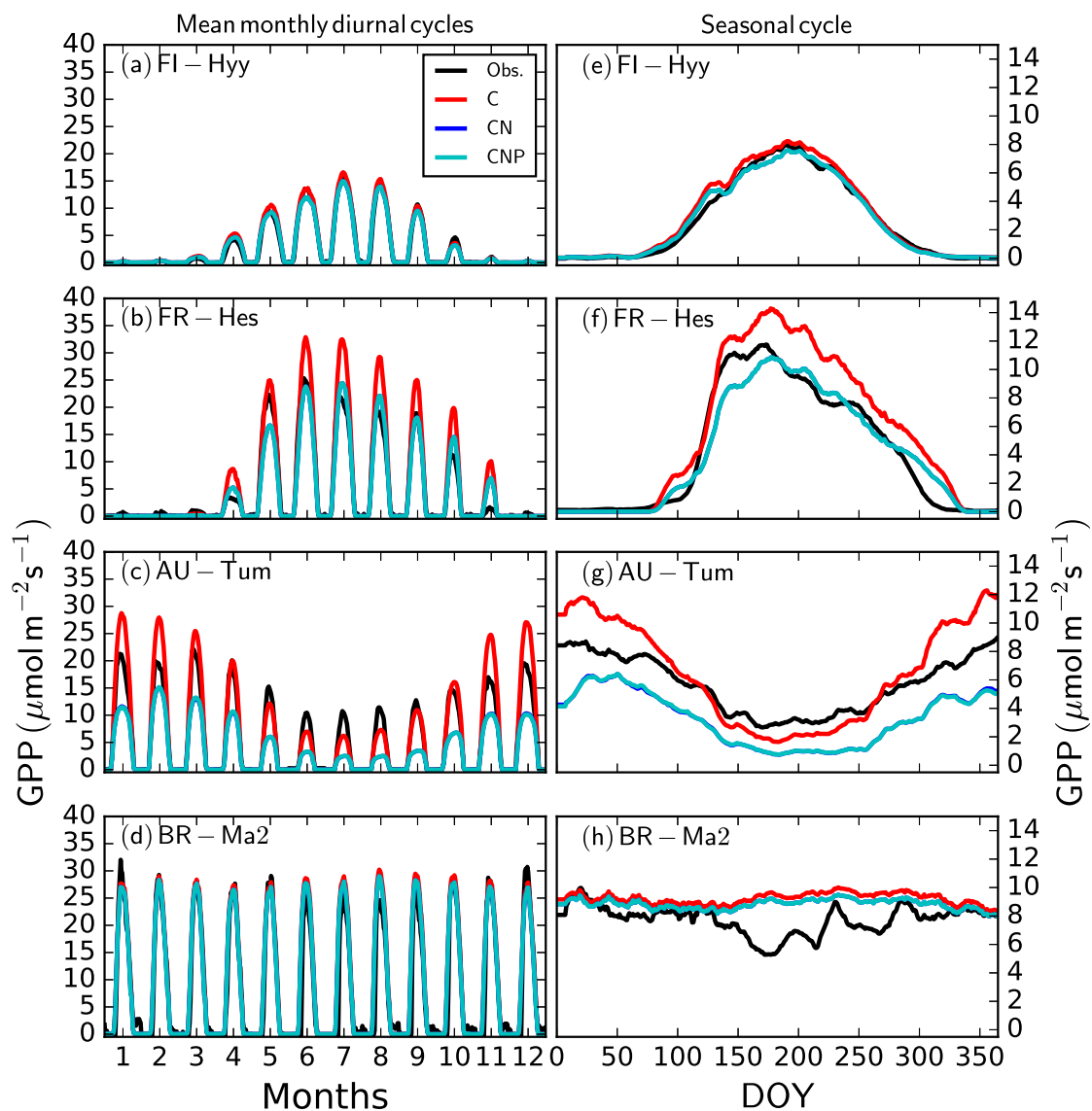
**Figure 3.** Simulated and observed mean monthly diurnal (a, b, c, d) and seasonal (e, f, g, h) cycles of gross primary production (GPP) at four FLUXNET sites (FI-Hyy, FR-Hes, AU-Tum, BR-Ma2, see Tab. A1) representing the major QUINCY PFTs (NE, BS, TeBE, and TrBE, respectively, see Tab. 1). 'Obs' correspond to micrometeorological observations. 'C', 'CN' and 'CNP' refer to the model simulations with C, C&N and C&N&P options enabled. Seasonal cycles have been smoothed by a 16-day running mean.
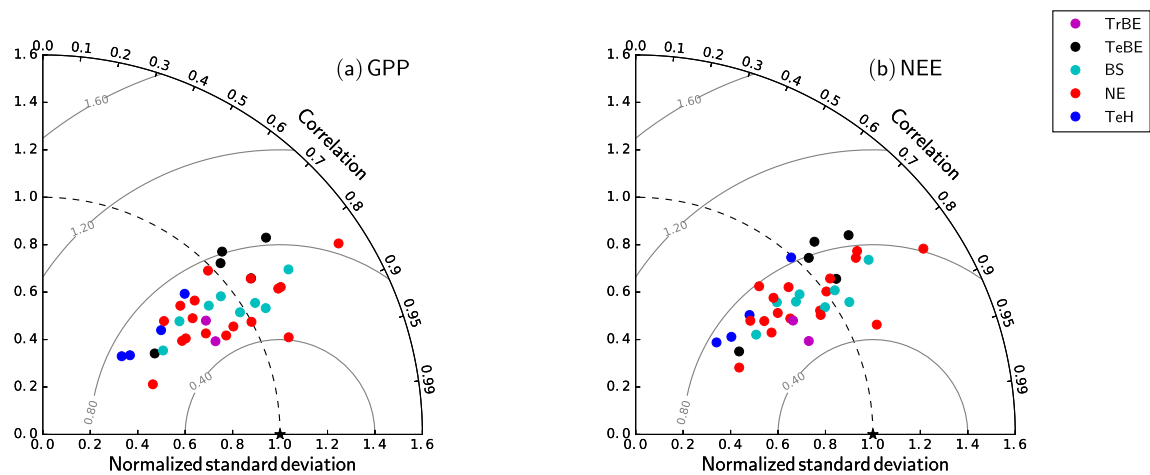
**Figure 4.** Taylor plots for gross primary production (GPP) and net ecosystem exchange (NEE) showing the model-data agreement for the FLUXNET sites used in this study (Tab. A1), separated according to the dominant plant functional type (Tab. 1). The standard deviation was normalized against the standard deviation of the observations for the corresponding variable. The grey lines correspond to the euclidean distance from the point of perfect model-data agreement, where both the normalised standard deviation and the correlation coefficient are 1.0, shown as a black star in the figure.
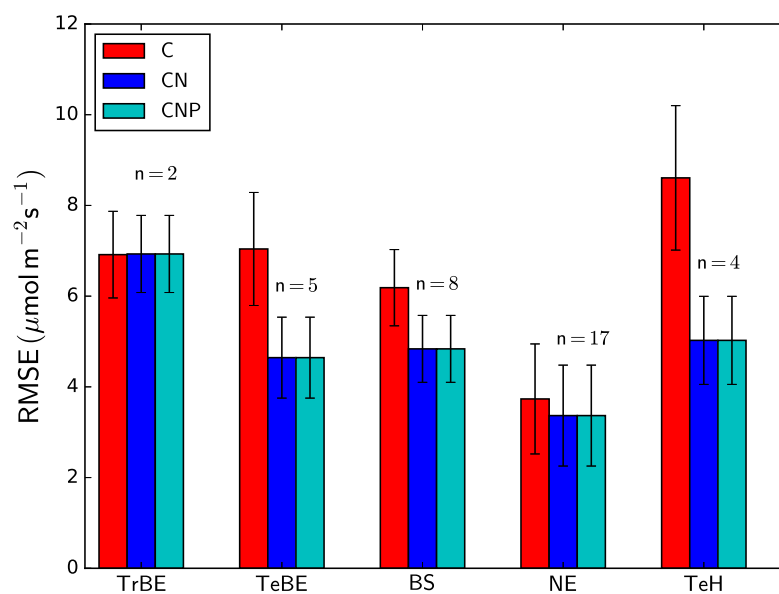
**Figure 5.** Root mean square error (RMSE) for simulated gross primary production (GPP) by dominant plant functional type (see Tab. 1). The number of sites used in the calculation of the PFT-specific RMSE value (n) is shown above the bars for each PFT. The error bars denote the standard deviation of the RMSE values of the different sites within each PFT. 'C', 'CN' and 'CNP' refer to the model simulations with C, C&N and C&N&P options enabled.
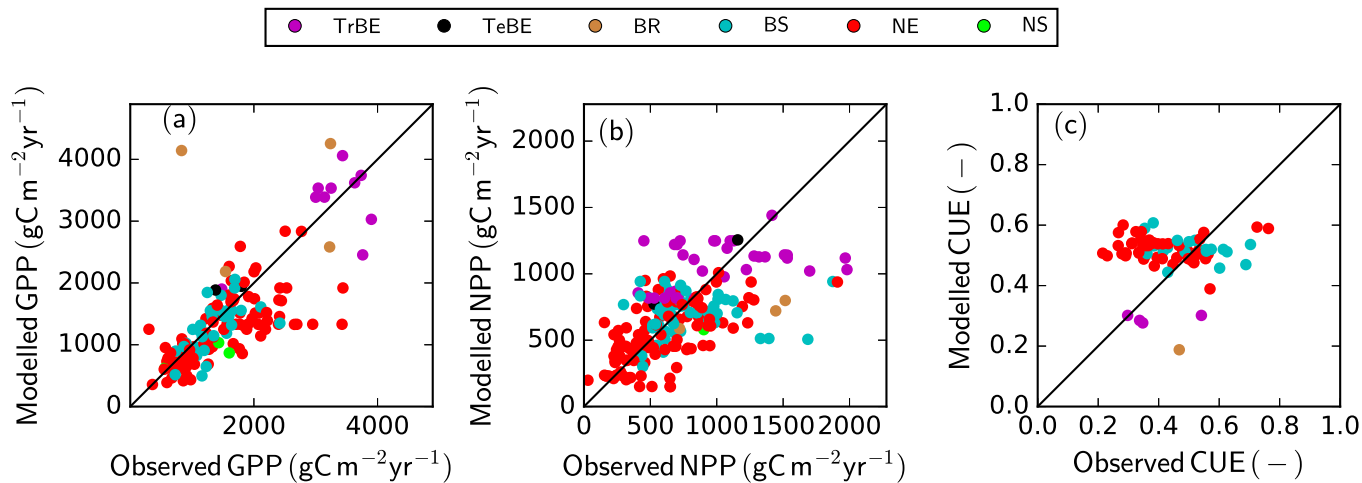
**Figure 6.** Simulated versus observed gross primary productivity (GPP) (a), net primary productivity (NPP) (b) and carbon use efficiency (CUE=NPP/GPP) (c) at GFDB sites against observations. For PFT abbreviations, see Table 1. Note that observations of GPP and NPP are not consistently available for all sites.
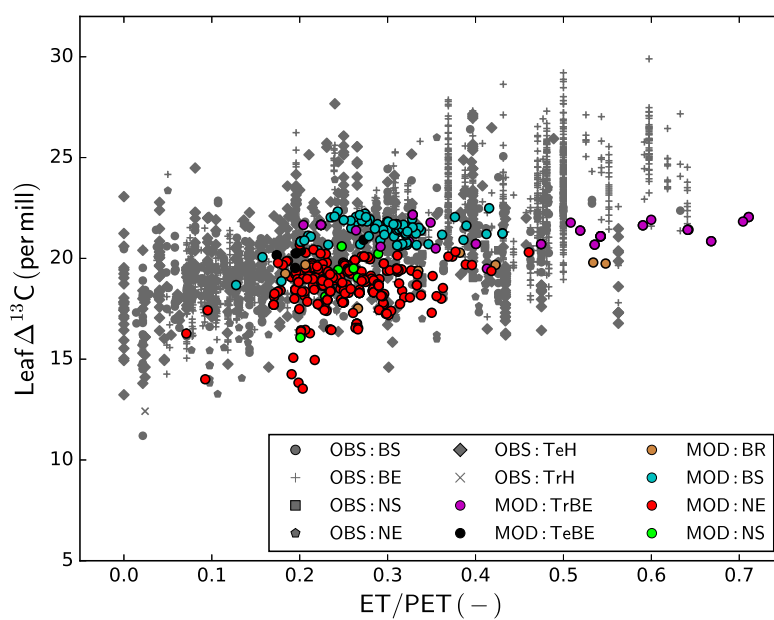
**Figure 7.** Observed and simulated leaf $\Delta^{13}$C. Observations are taken from the global database of (Cornwell et al., 2018b), simulations are derived from the GFDB set of sites (see Fig. 2). As there is no direct correspondence between data and model location, the data are plotted as a function of climatic water deficit, measured as the ratio of actual to potential evapotranspiration (ET/PET). For model PFT abbreviations, see Table 1.
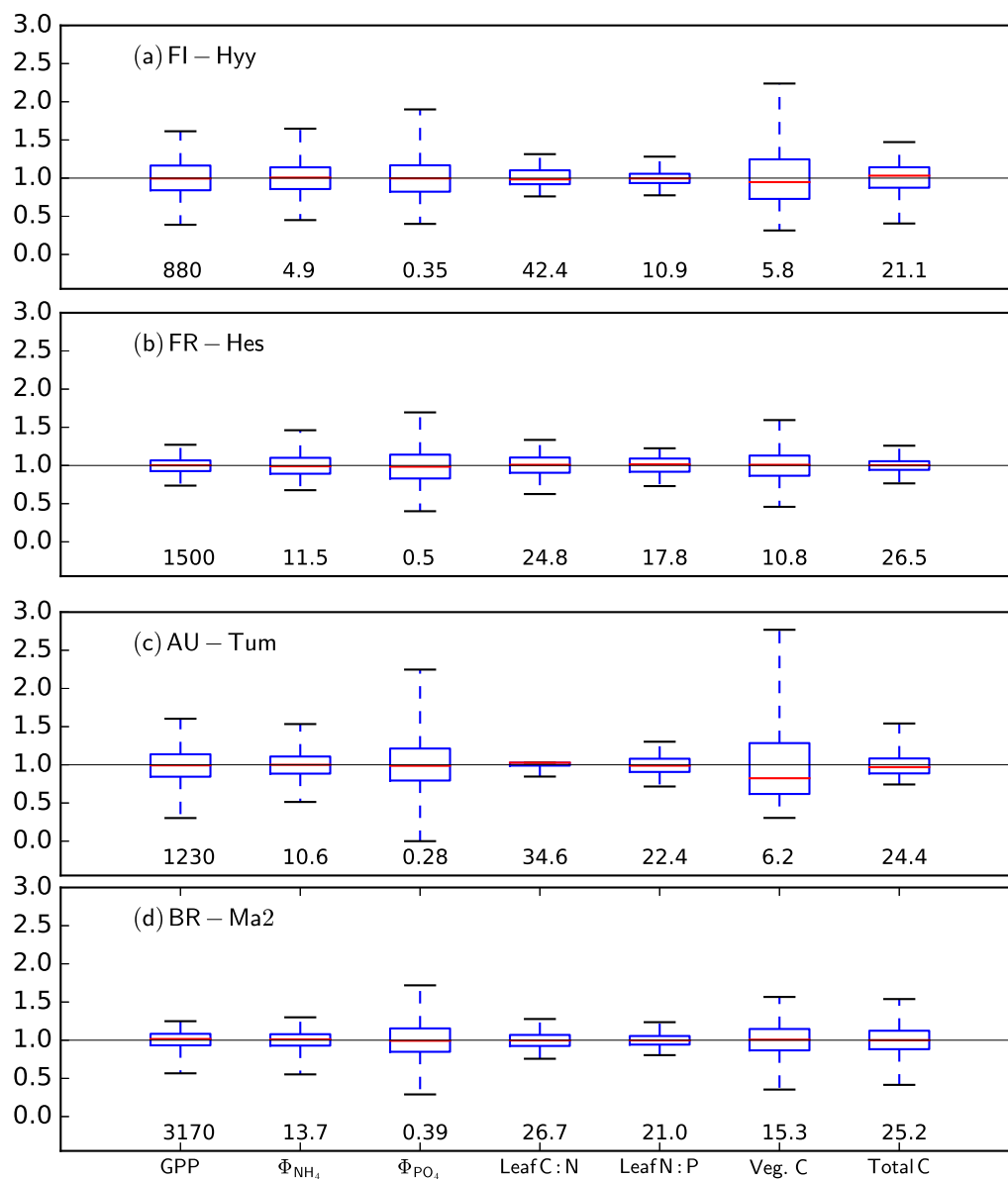
**Figure 8.** Median, inner-quartile range and absolute range of simulated gross primary production (GPP), net mineralisation of $NH_4$ ($\Phi_{NH_4}$) and $PO_4$ ($\Phi_{PO_4}$), leaf C:N and N:P, as well as vegetation C (veg. C) and total ecosystem C (up to a depth of 1m) obtained for the four FLUXNET sites in Fig. 3 using latin-hypercube sampling (n=1000) for 45 parameters. Values have been normalised to the ensemble mean, given as number for each site and variable, to improved readability.

**Table 1.** Description of plant functional types used in the model

| Number | Abbreviation | Description |
|--------|-------------|-------------|
| 1 | TrBE | Tropical broad-leaved evergeen |
| 2 | TeBE | Temperate broad-leaved evergreen |
| 3 | BR | (Tropical) broad-leaved rain deciduous (rain green) |
| 4 | BS | (Temperate & Boreal) Broad-leaved winter deciduous (summer green) |
| 5 | NE | (Temperate & Boreal) Needle-leaved evergreen (coniferous evergreen) |
| 6 | NS | (Temperate & Boreal) Needle-leaved winter deciduous (summer green) |
| 7 | TeH | C3 grass |
| 8 | TrH | C4 grass |

**Table 2.** The C, N, and P fluxes and stocks at four FLUXNET sites; as in Fig. 3. Values of stocks and fluxes are averaged over the years where $CO_2$ flux observations are available. All soil stocks are calculated for the topmost one meter. LAI and height represent the $90^{th}$ percentile of the timeseries.

| Variable | Unit | FI-Hyy | FR-Hes | AU-Tum | BR-Ma2 |
|---|---|---|---|---|---|
| **C stocks** | | | | | |
| Vegetation C | $kgC\ m^{-2}$ | 7.0 | 11.1 | 5.0 | 16.4 |
| Litter C | $kgC\ m^{-2}$ | 3.2 | 3.0 | 4.3 | 2.6 |
| Soil organic C | $kgC\ m^{-2}$ | 13.3 | 12.9 | 14.5 | 7.4 |
| **N stocks** | | | | | |
| Vegetation N | $gN\ m^{-2}$ | 38.0 | 83.1 | 31.7 | 105.4 |
| Litter N | $gN\ m^{-2}$ | 19.2 | 25.1 | 47.5 | 23.8 |
| Soil organic N | $gN\ m^{-2}$ | 1427 | 1397 | 1547 | 794 |
| Soil inorganic N | $gN\ m^{-2}$ | 0.42 | 0.56 | 0.14 | 0.28 |
| **P stocks** | | | | | |
| Vegetation P | $gP\ m^{-2}$ | 3.68 | 5.45 | 1.75 | 5.27 |
| Litter P | $gP\ m^{-2}$ | 1.86 | 1.55 | 2.48 | 1.24 |
| Soil organic P | $gP\ m^{-2}$ | 101.9 | 99.4 | 110.6 | 56.7 |
| Solute & labile P | $gP\ m^{-2}$ | 52.7 | 38.7 | 6.19 | 86.7 |
| Sorbed P | $gP\ m^{-2}$ | 65.0 | 41.5 | 6.81 | 67.5 |
| Occluded P | $gP\ m^{-2}$ | 201.6 | 187.7 | 72.5 | 290.2 |
| Primary P | $gP\ m^{-2}$ | 168.5 | 175.0 | 34.7 | 530.9 |
| **Vegetation characteristics** | | | | | |
| LAI | - | 4.8 | 6.0 | 3.7 | 6.8 |
| Height | m | 8.6 | 11.4 | 6.5 | 14.4 |
| Leaf C:N | - | 41.5 | 23.9 | 34.8 | 25.6 |
| Leaf N:P | - | 11.3 | 18.2 | 21.4 | 21.0 |
| **C fluxes** | | | | | |
| GPP | $gC\ m^{-2}\ yr^{-1}$ | 1020 | 1559 | 1230 | 3344 |
| NPP | $gC\ m^{-2}\ yr^{-1}$ | 536 | 763 | 662 | 1019 |
| **N fluxes** | | | | | |
| N uptake | $gN\ m^{-2}\ yr^{-1}$ | 6.25 | 12.76 | 12.09 | 15.32 |
| Net mineralisation | $gN\ m^{-2}\ yr^{-1}$ | 5.37 | 11.51 | 11.24 | 14.14 |
| N deposition | $gN\ m^{-2}\ yr^{-1}$ | 0.66 | 1.69 | 0.26 | 0.24 |
| Asymbiotic N fixation | $gN\ m^{-2}\ yr^{-1}$ | 0.40 | 0.01 | 0.68 | 1.65 |
| N gas loss | $gN\ m^{-2}\ yr^{-1}$ | 0.15 | 0.33 | 0.04 | 0.39 |
| N leaching loss | $gN\ m^{-2}\ yr^{-1}$ | 0.06 | 0.14 | 0.05 | 0.33 |

**Table 2.** The C, N and P stocks and fluxes at four FLUXNET sites (continued).

| Variable | Unit | FI-Hyy | FR-Hes | AU-Tum | BR-Ma2 |
|---|---|---|---|---|---|
| **P fluxes** | | | | | |
| P uptake | gP m$^{-2}$ yr$^{-1}$ | 0.58 | 0.76 | 0.59 | 0.74 |
| Net mineralisation | gP m$^{-2}$ yr$^{-1}$ | 0.37 | 0.49 | 0.32 | 0.40 |
| Biochemical mineralisation | gP m$^{-2}$ yr$^{-1}$ | 0.14 | 0.19 | 0.22 | 0.27 |
| P deposition | mgP m$^{-2}$ yr$^{-1}$ | 2.12 | 6.46 | 1.20 | 1.24 |
| P leaching loss | mgP m$^{-2}$ yr$^{-1}$ | 0.21 | 0.53 | 0.27 | 2.66 |
| Weathering | mgP m$^{-2}$ yr$^{-1}$ | 14.5 | 17.6 | 20.4 | 44.6 |

**Table 3.** The ten most important parameters (P) determining model uncertainty at four FLUXNET sites (FI-Hyy, FR-Hes, AU-Tum, BR-Ma2, as in Figs. 3 and 8), and reference to the respective parameter description table in the Supplementary Materials (T). Overall importance of parameters is measured by calculating the RPCC for each output variable, and then calculating the mean of the absolute RPCC values across GPP, net N/P mineralisation, vegetation and ecosystem C, as well as leaf C:N:P, weighted by the uncertainty contribution of these model outputs.

| | FI-Hyy | | FR-Hes | | AU-Tum | | BR-Ma2 | |
|---|---|---|---|---|---|---|---|---|
| Rank | P | T | P | T | P | T | P | T |
| 1 | $k_0^{struc}$ | S2 | $T_{opt,decomp}$ | S4 | $T_{opt,decomp}$ | S4 | $k_0^{struc}$ | S2 |
| 2 | $T_{opt,decomp}$ | S4 | $k_{rp}$ | S3 | $\eta_{C,litter \to fast}$ | S4 | $k_{fn}^{chl}$ | S2 |
| 3 | $k_{fn}^{chl}$ | S2 | $\eta_{C,litter \to fast}$ | S4 | $\eta_{C,fast \to slow}$ | S4 | $\chi_{leaf}^{C:N}$ | S7 |
| 4 | $\eta_{C,litter \to fast}$ | S4 | $\eta_{C,fast \to slow}$ | S4 | $k_0^{struc}$ | S2 | $k_{rp}$ | S3 |
| 5 | $\eta_{C,fast \to slow}$ | S4 | $k_0^{struc}$ | S2 | $k_{rp}$ | S3 | $f_{resp,maint}^{non-woody}$ | S3 |
| 6 | $a_{chl}^n$ | S2 | $\tau_{slow}^{base}$ | S4 | $\tau_{slow}^{base}$ | S4 | $T_{opt,decomp}$ | S4 |
| 7 | $k_{rp}$ | S3 | $k_{latosa}$ | S7 | $sla$ | S7 | $v_{cmax}^n$ | S2 |
| 8 | $\chi_{leaf}^{N:P}$ | S7 | $\chi_{root}^{C:N}$ | S3 | $\chi_{SOM_{slow}}^{N:P}$ | S4 | $K_{demand}^{half,N}$ | S4 |
| 9 | $\chi_{root}^{C:N}$ | S3 | $T_{opt,nit}$ | S4 | $\chi_{SOM_{slow}}^{C:N}$ | S4 | $a_{chl}^n$ | S2 |
| 10 | $K_{demand}^{half,P}$ | S4 | $sla$ | S7 | $k_{latosa}$ | S7 | $k_{latosa}$ | S7 |